Chain End Segregation at Polymer Thin Film Surfaces

by

Thomas Francis Schaub, Jr.

B.S., Engineering Physics
State University of New York at Buffalo, 1993

Submitted to the Department of Materials Science and Engineering
in partial fulfillment of the requirements for the degree of

Master of Science in Materials Science and Engineering

at the

MASSACHUSETTS INSTITUTE OF TECHNOLOGY

June 1995

Author .....
Department of Materials Science and Engineering
May 12, 1995

Certified by .....
Anne M. Mayes
Class of '48 Assistant Professor of Polymer Physics
Thesis Supervisor

Accepted by .....
Carl V. Thompson II
Professor of Electronic Materials
Chair, Departmental Committee on Graduate Students

Chain End Segregation at Polymer Thin Film Surfaces

by

Thomas Francis Schaub, Jr.

Submitted to the Department of Materials Science and Engineering
on May 12, 1995, in partial fulfillment of the
requirements for the degree of
Master of Science in Materials Science and Engineering

Abstract

Chain end segregation, the localization of a high polymer's chain-end repeat units at a surface, has been observed and modelled in this thesis. A series of polystyrene samples ranging in molecular weights from 4k to 90k were anionically synthesized and terminated with a functionalized silane group containing an oligotetrafluoroethylene tail. After characterization, these samples formed the basis for two related avenues of experimentation. First, x-ray photoelectron spectroscopy and neutron reflectivity (NR) studies were performed on thin films of neat end-functionalized polymer samples to measure chain end segregation. Complete segregation of chain ends to the air surface and substrate interface was seen in films less than $4R_G$ in thickness. Next we explored the possibility of utilizing chain end segregation as a means of controlling the properties of a polymer surface. AB/A blends consisting of end-modified polymers and high molecular weight polystyrenes were studied using NR as a function of the blend concentration. Our results indicate that a high fraction of end-modified polymer localizes near the surface. To complement both sets of studies, contact angle measurements were taken to observe what effect these structural changes have upon surface properties. In each case, the surface energy is found to be lower for higher surface concentrations of chain ends. Results from a free energy model of the blend systems are compared with the experimental results from the blend studies.

Thesis Supervisor: Anne M. Mayes
Title: Class of '48 Assistant Professor of Polymer Physics

Acknowledgments

The last two years at MIT have been an exciting part of my life. I'm grateful that I've been able to draw upon the wealth of knowledge that the people who make up the MIT community have to offer. For their support, both professional and personal, I would like to acknowledge the people without whom this thesis would not have materialized:

To Prof. Anne Mayes whose talent and dedication have never ceased to amaze me. As one of Anne's first graduate students, I think we've both learned alot; at least she can't say I left her with any more gray hairs for her efforts.

To Drs. Greg Kellogg and Bruce Carvalho who shared their wisdom freely. Their input for this work was virtually continuous; 20% is on the way guys.

To Dave Walton who taught me alot about how to use computers. Maybe Andersen got things mixed up.

To Ish Modak who has been a special and integral part of my life for the last year. Her constant encouragement kept me going at times I didn't think I'd make it.

To my parents and family whose generous love gives me the confidence I need. Thank you for the freedom to pursue my aspirations.

To the many others who have played important roles in conjunction with my experience here at MIT, especially: Neal Mitra, Roland Ayala, Mark Brillhard, Doris Lee, Jeff Baur, Jason Gratt, Jimmarie Ramos, and Jim Bandy.

Contents

List of Figures

List of Tables

Chapter 1

Introduction

When considering the suitability of a material for a particular design application, some of the most important factors to be taken into account are the surface properties of the material. There are at least two reasons why special attention must be given to a material's surface properties: first, the properties desired at the surface are often specific and distinct from the bulk properties of the material; and second, materials may exhibit different structural characteristics near a surface which will affect the material's properties. Examples of properties affected by polymer surface structure include adhesion, wettability, friction, permeability, stain resistance, gloss, corrosion, surface electrostatic charging, cellular recognition, and biocompatibility [1]. From this perspective it is easy to understand why such a large volume of research has been directed at understanding the nature by which surfaces modify polymer structure and at using this knowledge to control the surface properties exhibited by polymers.

Classically, control of a material's surface properties has been achieved by modification of the surface through various chemical or physical processes. The most common surface modification techniques include plasma treatment [2, 3], surface grafting [4, 5], chemical reaction [2, 6], vapor deposition of metals [7], and flame treatment [8]. Such kinetically governed reaction mechanisms however, allow relatively little control over the final surface composition and structure. Other techniques for controlling surface properties include incorporating

small molecules or oligomeric additives which migrate to the polymer surface [9]. Because they are not strongly bound to the polymeric matrix however, such additives may compromise the polymer's bulk physical properties by diffusing away from the surface; they may also be removed altogether by evaporation, for example.

One recent innovation in the attempt to gain careful control of the surface composition and properties, while maintaining the structural integrity of the bulk matrix, has been to chemically synthesize polymers which have "surface specific" tails of various functionalities [10]. Preliminary results indicate that using end-functionalized polymers with low energy fluorocarbon tails enhances the surface concentration of these chain ends; more studies are needed however. These end-modified materials have also been employed in the synthesis of high molecular weight lipophilic polymers — such as polystyrene, poly(methyl methacrylate), and styrene-butadiene rubber — using supercritical carbon dioxide (CO_2) as a solvent, whereby the fluorocarbon moiety acts to stabilize the growing chains in the CO_2 [11, 12, 13]. The attractiveness of this synthetic route from an environmental standpoint could ultimately lead to wide scale production of such end-functionalized polymers, making their application as surface modification agents commercially feasible.

The mechanism behind this concept of surface control is explained by understanding the role a surface, or non-interacting interface, plays in modifying the enthalpic and entropic forces governing a polymer's behavior near an impenetrable boundary. In the bulk — in the absence of strong enthalpic interactions — polymer chains typically take on a so-called random coil conformation, where the physical orientation of each repeat unit along the chain's backbone is essentially uncorrelated with the orientations of the chain's other repeat units. The presence of a surface, however, places tight constraints upon the conformations of chains near the surface such that the random coil conformation is perturbed. To alleviate this entropically unfavorable situation and lower the overall free energy of the system, it has been predicted [14] that polymer chains in the

vicinity of the surface will segregate their chain ends to the boundary, thereby avoiding the unnecessary entropic penalty.

An argument which may be made against surface control via end-modified polymers is that although it is technologically possible to synthesize such polymers, the cost of doing so would be prohibitively expensive. To circumvent this problem, one alternative is to blend the high-cost, end-functionalized polymers with low-cost, widely available commodity plastics, referred to as AB/A blends. The anchoring portion of the end-functionalized polymer is chosen to match the commodity plastic, while the end-functionalized tail is selected to deliver the desired surface properties. A recent study on block copolymers [15] suggests only small amounts of specially synthesized polymers may be needed to obtain appreciable levels of surface enrichment of the low surface energy component, and hence control of the surface properties.

The present work explores two aspects of chain end segregation. In each case the primary vehicle by which chain end segregation phenomena are investigated is a series of anionically synthesized end-functionalized (or end-modified) polymers of various molecular weights. The first avenue examined is the dependence of molecular weight on the degree of chain end segregation. To study this relationship, three experimental techniques are used: x-ray photoelectron spectroscopy (XPS), neutron reflectivity (NR), and contact angle measurements. The second avenue pursued is the usage of end-modified polymers in AB/A blends. To undertake this examination, a theoretical description of the systems being studied is first developed and used to help anticipate experimental results. Experiments are then conducted using NR to assess and measure the extent to which end-modified polymers segregate as a result of their low surface energy tails.

This thesis is divided into seven chapters. Chapter 2 contains an in-depth review of previous works performed on chain end segregation and its related topics. Chapter 3 presents a discussion and results of a free energy model developed and executed to predict the degree of chain end segregation in AB/A blends.

Chapter 4 describes the experimental procedures used in this investigation, including the anionic synthesis and characterization of the end-functionalized polymers by gel permeation chromatography, differential scanning calorimetry, and fourier transform infrared spectroscopy; additionally, basic explanations of x-ray photoelectron spectroscopy, contact angle measurement, and neutron reflectivity analyses are provided; lastly, details of the techniques used in the sample preparation are given. Chapter 5 presents the results and discussion of this effort. Chapter 6 is a summary of the conclusions to be drawn from these studies. Finally, chapter 7 suggests directions which future studies of chain end segregation may take. Appendix A includes the Fortran source code for the free energy model presented in chapter 3. Appendix B provides GPC data as a supplement to chapter 4. Appendix C illustrates NMR spectra for the end-modified systems synthesized for this study.

Chapter 2

Chain End Segregation

2.1 Evidence for Chain End Segregation

In bulk, amorphous high polymers typically take the conformation of a random coil. Physically this model is essential in explaining many polymer phenomena, such as the dynamic and thermodynamic properties of polymer melts [16]. Polymer chains having random coil conformations can be characterized by the most probable end–to–end distance R_G, also known as the root mean square (rms) end–to–end distance, given by equation 2.1, where N is the number of chain segments and a is the statistical segment length.

$$R_G = N^{1/2}a \tag{2.1}$$

In the vicinity of a surface or non-interacting interface, however, the random coil conformation is perturbed. To minimize the loss in conformational entropy, polymer molecules within one rms distance of the surface may localize their chain ends to the surface (see figure 2-1) [14] and thereby avoid the required "reflection" at the material boundary.

DeGennes has explored this concept in greater detail, and has expressed this tendency in terms of a preferential attraction between the terminal (chain end) groups and the free surface [17]. The central parameter, u, in his model is

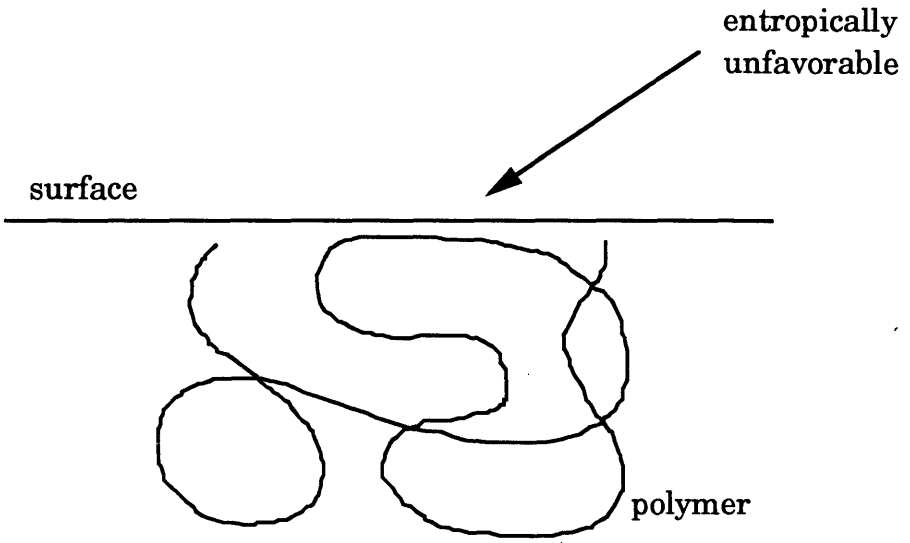

Figure 2-1: Perturbed polymer conformation at a surface

given by:

$$u = \frac{\Delta a^2}{k_b T} \tag{2.2}$$

where Δ is the difference in surface tensions, $\gamma_\infty - \gamma_{end}$, between a hypothetical chain with no ends and a real chain's terminal groups, a^2 is the surface area per monomer, and the product $k_b T$ is the thermal energy at temperature T. According to his explanation, three regimes of behavior can be delineated depending on the magnitude of u. Figure 2-2 presents a brief schematic to help illustrate the nature of the behavior endemic to each regime:

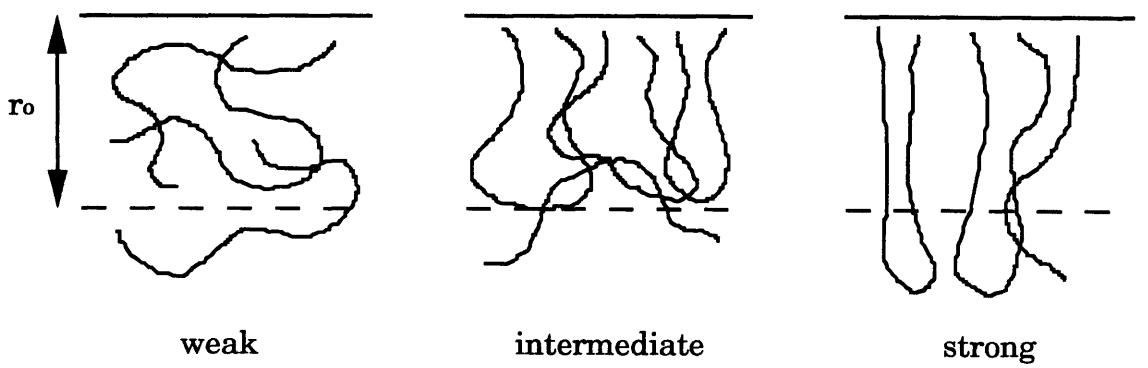

Figure 2-2: The three regimes of chain end segregation

Regime I ($u \ll 1$): In the weak regime the surface does not perturb the chains, hence the random coil conformation is not compromised. The surface volume fraction of chain ends is effectively equal to the bulk ϕ_β, and the surface tension is $\gamma_\infty - \Delta\phi_\beta$.

Regime II ($u \approx 1$): In the intermediate regime all chain ends within R_G of the surface will be localized at the surface. From this it follows that the concentration of chain ends near the surface, ϕ_s, will equal $(R_G/a)\phi_\beta$.

Regime III ($u > 1$): In the strong segregation regime Δ is of such magnitude that chains will stretch to accomodate more chain ends per unit surface area. The increased concentration of chain ends at the surface is limited by the increase in elastic free energy of the chains near the surface.

Theoretically, chain end segregation has been predicted on the basis of mean-field calculations, as well as molecular dynamics and Monte Carlo simulations. Mean-field results for the case of end-modified polymers predict a preferential adsorption of the surface active "head", even in the absence of an interaction parameter (*i.e.* $\chi_s = 0$) [18]. This finding was explained on entropic grounds, as chain end segments have fewer constraints than mid-chain segments. The molecular dynamics results showed an excess of end groups in the region nearest the gas phase (*i.e.* the outermost region) with an excess of "middle" groups in the region immediately beneath the first. The authors suggest that a middle group in the outermost region is energetically unfavorable and may force the chain into an unfavorable "horseshoe" conformation [19, 20]. Finally, Monte Carlo results showed the occupancy of end groups in the first sublayer next to an interface more than twice as large as the bulk average [21].

Experimental evidence for the segregation of chain ends to the surface of polymer melts is currently limited. In one study, Meyers et al. used atomic force microscopy to probe the surface of amorphous polystyrene (PS) systems of various molecular weights [22]. Surface patterns were observed analogous to Schallamach abrasion "waves" which form on the surface of rubbery materials.

These results were interpreted as evidence that the nature of the PS surface is elastic, even though the bulk glass transition falls at around 110°C. The authors further noted a clear molecular weight dependence in the characteristic spacing of the observed surface modulations. These results suggest a depression of the surface T_g as evidenced by the lower elastic modulus at the surface relative to the bulk. Though not explicitly stated, chain end segregation could account for the author's findings [23].

A more direct verification for chain end segregation has recently been reported by Zhao et al. [24] using neutron reflectivity (NR). Their study utilized a deuterated polystyrene (dPS)/PS/dPS triblock of M_w = 65.6k. Experimental results indicated that the labelled dPS ends did in fact segregate to the surface. The authors claim that the best model to account for their data indicated a two-times excess of chain ends at the free surface. This result is questionable however, since it did not properly account for a depletion region beneath the surface excess region where a paucity of chain ends would be expected had chain end segregation actually occurred.

In another study, Botelho do Rego et al. [25], used high resolution electron energy loss spectroscopy (HREELS), a vibrational spectroscopy technique sensitive to isotopic substitutions in polymer chains, to measure the relative abundance of triblock components near the surface. A M_n=10.4k dPS/PS/dPS polymer was used, with each of the dPS segments being approximately 2 repeat units in length. In HREELS the recoiling energy of inelastically backscattered electrons is measured such that peaks appear in the spectra at energies corresponding to the molecular vibrational energies of the material being probed. An end-segment concentration of twice the bulk value was reported near the surface, followed by a depletion region, such that the total penetration depth probed by the electron beam was approximately 10$\mathring{A}$.

In a related work [26], Affrossman et al. attempted to isolate the impact of the chemical nature of the chain ends upon surface segregation. In addition to using the dPS/PS/dPS triblock from [25], a M_n=10.4k PS/dPS/PS triblock

was synthesized having PS tails each approximately 3 segments in length. Using static secondary ion mass spectroscopy a 300% surface excess of the PS ends in the PS/dPS/PS triblock, and a 400% surface excess of dPS ends in the dPS/PS/dPS triblock was observed. Since the complementary results rule out a large surface energy difference between perdeuterated and hydrogenated materials, the authors conclude from this experiment that there is a natural tendency for chain ends to segregate to the surface.

Finally, Elman et al. [10] recently examined the effects of polymer functionalization upon chain end segregation. In their study anionic synthesis was used to make PS/dPS diblocks with high energy (repulsive) end groups, low energy (attractive) end groups, and neutral (control) end groups. Their results qualitatively suggest a depletion of the high energy carboxylic acid end groups and a surface excess of the low energy fluorocarbon chain end groups in the respective experiments. The authors further noted the importance of the initiator fragment capping the chain at the end opposite the terminal group, suggesting that surface adsorption of the fragment occurs in all three cases.

2.2 Surface Properties: Chain End Segregation

The presence of chain ends affects both bulk and surface properties. In bulk, measurements on polymeric materials have shown that many physical properties, such as density and yield strength, obey a scaling relation of the following form [27, 28]:

$$P = P_\infty - k_b/M_n \ . \tag{2.3}$$

In this relation P is the bulk property of concern, P_∞ is the bulk property of a hypothetical infinite molecular weight polymer, k_b is a parameter which depends on the specific polymer's properties and M_n is the number average molecular weight [29]. This relationship captures the effect which chain ends have upon the polymer's bulk properties. Since the volume fraction of chain

ends, ϕ_β, in the bulk is $2/N$, the larger the molecular weight, the smaller the contribution made by chain ends to the property.

A relationship similar in form to equation 2.3 has been observed for surface tension [30, 31, 14]:

$$\gamma = \gamma_\infty - k_\sigma M_n^{-x} \tag{2.4}$$

where γ is the surface tension, γ_∞ is the extrapolated surface tension of an infinite molecular weight polymer where the effects of chain ends are negligible, and k_σ is a material parameter. The scaling exponent, x, has been found to have a value on the order of 2/3 depending on the polydispersity and molecular weight of the system [29, 32]. The fact that the exponent is less than 1 suggests that chain ends are attracted to the surface thus enhancing their contribution to this surface property.

The predicted increase in surface concentration of chain ends for systems in the intermediate and strong regimes may also have important consequences on other surface properties. Mayes has suggested that an excess concentration of chain ends will lead to a depression in the glass temperature of the surface region, $T_{g,s}$ [23]. Assuming intermediate regime behavior for a system, ϕ_s can be expressed in terms of the number of chain segments by substituting for R_G and ϕ_β in the ϕ_s relationship

$$\phi_s = (\frac{R_G}{a})\phi_\beta = \frac{(N^{1/2}a)}{a}\frac{2}{N} = \frac{2}{N^{1/2}}. \tag{2.5}$$

Whereas the bulk concentration of chain ends scales as N^{-1}, the surface concentration scales as $N^{-1/2}$, and the surface glass temperature depression is expressed as follows:

$$\Delta T_{g,s} = T_{g,\infty} - T_{g,s} = C/N^{1/2}\ . \tag{2.6}$$

The magnitude of this depression can be quite sizable even for high polymers, and warrants careful consideration when designing applications with a hard

surface in mind.

Another example of how chain end segregation can be used to control surface (and interfacial) properties was recently presented by Norton et al. [33]. Their study utilized a series of carboxylic acid terminated deuterated polystyrene (dPS-COOH) samples to enhance adhesion at a thermoset-thermoplastic interface. Since the end-functionalized tail grafts to the epoxy resin, a large increase in fracture toughness may be expected to result. Their studies showed that for the optimized surface density of dPS-COOH, an increase of over 20 times the bare interfacial fracture toughness was achieved.

Chapter 3

Free Energy Model

3.1 Model Development

A free energy model was developed to describe the segregation of chain ends at a surface or non-interacting interface in AB/A polymer blend films. The approach taken in developing this phenomenological model is similar to that followed in the development of models for the formation of micelles [34, 35]. The system modelled has two components, an end-modified polymer (AB) of N total segments, with short, low surface energy tails (represented as B), and a homopolymer (A) with N_h segments. The localization of the low energy chain ends at the surface is assumed for the end-modified chains in the near-surface region. The free energy of the system is constructed with reference to a bulk state where the two components are completely separated.

The overall expression of the free energy which describes this system has the following form:

$$F_{total} = F_{surf} + F_{mix}$$

where F_{surf} is the free energy of the near-surface region, and F_{mix} is the Flory–Huggins free energy of mixing for the two polymers outside the near-surface region. Figure 3-1 depicts the geometry assumed for this model. At the surface, the low surface tension tails are expected to localize, creating a near-surface

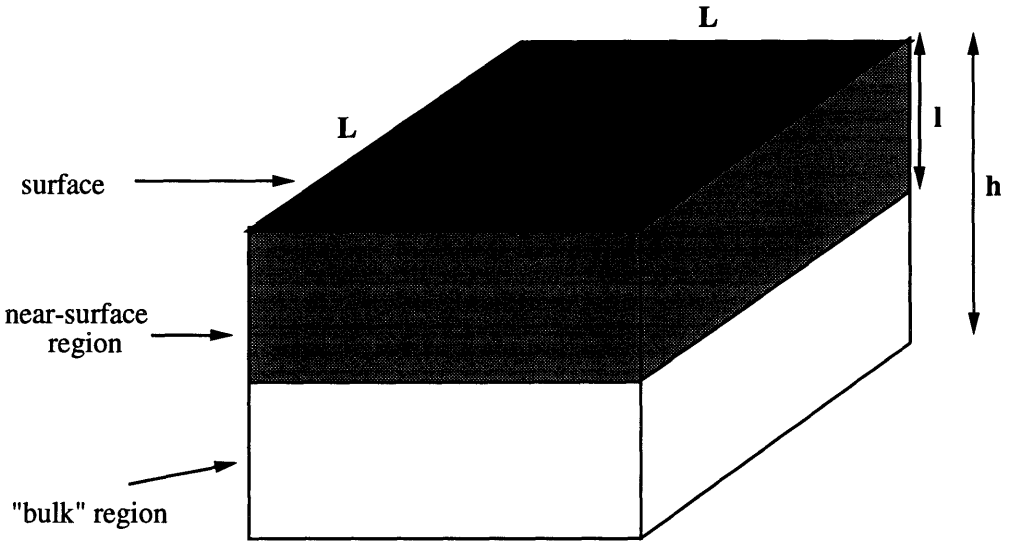

Figure 3-1: Schematic illustration of the free energy model for AB/A blends

region where the anchored chains and the matrix homopolymer are expected to mix. In the bulk region, end-modified polymers which do not segregate to the surface intermix with unmodified homopolymers.

The free energy F_{surf} of the near-surface region can be broken down into three components as follows:

$$F_{surf} = A_i\sigma + \mathcal{F}_d + \mathcal{F}_m \tag{3.1}$$

$A_i\sigma$ represents the contribution from the interfacial tension, $\mathcal{F}_d$ represents the contribution from the deformation of the polymer chains, and $\mathcal{F}_m$ represents the Flory–Huggins free energy of mixing for the AB and A polymers in the near-surface region.

The first term derives from the difference in surface tensions between a chain end and a main chain segment. The free energy expression for $A_i\sigma$ is equal to the surface area, L^2, multiplied by the thermal energy k_bT, multiplied by the surface fractions covered by each of the system's three components, *i.e.* end-modified chain end segments, end-modified anchoring segments, and homopolymer main

chain segments. Using data taken from [9], this is expressed as:

$$k_bTL^2\{\eta\gamma_{A_{AB}}(\frac{L^2-2pa^2}{L^2})+(1-\eta)\gamma_{A_A}(\frac{L^2-2pa^2}{L^2})+0.803\frac{2pa^2}{L^2}\} \tag{3.2}$$

where η is the fraction of A monomer in the near surface region from end-modified polymer, $\gamma_{A_{AB}}$ is the surface tension of the end-modified polymer's A block, $2pa^2$ is the portion of the surface covered with end-modified tails, and γ_{A_A} is the surface tension of the A homopolymer. Captured in this term is the tendency for the system to lower its free energy by localizing the lower surface tension B component of the end-modified polymer to the surface. Also incorporated in the model through this term is the dependence of the surface tension on the molecular weight of the end-modified polymer and homopolymer; from equation 2.4 the molecular weight dependence can be expressed as:

$$\gamma_{A,i}=\gamma_{A,\infty}-k_\sigma M_{n,i}^{-2/3}. \tag{3.3}$$

The next term, $\mathcal{F}_d$, is the deformation term. Deformation energy results from a contraction or elongation of the end-modified chains from their unperturbed, random coil dimension. The specific form of this term is given as:

$$k_bTp[\frac{3}{2}\frac{l^2}{fNa^2}+\frac{\pi}{6}\frac{fNa^2}{l^2}] \tag{3.4}$$

where fN is the number of statistical segments in the A block of the end-modified polymer. This term is needed in part to counterbalance the first term; while a lower free energy can be achieved by localizing chain ends to the surface, a point is reached whereby chains must stretch to accomodate more ends. This is a very unfavorable conformation for individual chains to assume, and in the second regime the savings in free energy is not sufficient to overcome such a high entropic penalty.

The last contribution to the near-surface free energy, $\mathcal{F}_m$, is the mixing entropy between homopolymer and anchoring chains of the end-modified polymer

in the near-surface region, given as:

$$\frac{L^2 l k_b T}{a^3}\{\frac{\eta}{N_A}\ln\eta + \frac{(1-\eta)}{N_h}\ln(1-\eta)\} \tag{3.5}$$

where l is the thickness of the near-surface region, N_A is the number of statistical segments in the anchoring portion of the end-modified polymer, and N_h is the size of the homopolymer. The mixing entropy is increased by increasing the amount of homopolymer in the near-surface region. If, however, this concentration becomes too large, the A blocks will be elongated, which is energetically unfavorable. Also, with increasing homopolymer fraction, the surface coverage of low energy tails decreases.

A complete model must allow for the possibility that not all end-modified chains will segregate to the near-surface region. To account for this, F_{mix}, the Flory-Huggins free energy of mixing between the homopolymer and end-modified chains remaining outside the near-surface region, is included in the total free energy; it has the following form:

$$F_{mix} = k_b T \Omega(1-\varphi\gamma\Lambda)\{\frac{\varphi_1}{N}\ln\varphi_1 + \frac{(1-\varphi_1)}{N_h}\ln(1-\varphi_1)\} \tag{3.6}$$

where φ_1 is the concentration of end-modified polymer in the bulk region, $\varphi\gamma\Lambda$ is the volume fraction of the system occupied by the near-surface region, and Ω is the total number of monomers in the system. Note that the mathematical form of this term is identical to that of equation 3.5; this follows from the fact that both contributions to the total free energy arise from the same physical basis, the arguments are changed to accurately depict the components being mixed.

In order to minimize the free energy of the system for a given set of parameters, more information is needed. One assumption which can be made is that the material has a constant density, or in other words, that the system is incompressible. In making this statement the assumption is also made that both the chain end and main chain units have the same persistence length, or effec-

tively the same size. Strictly speaking this is not a fully accurate assumption, but given the small portion of the system which is composed of the modified end units, the error is minimal. Thus, incompressibility can be quantitatively stated as follows:

$$\Omega a^3 = L^2 h \tag{3.7}$$

where Ω represents the total number of monomers in the system, and h represents the thickness of the system as shown in figure 3-1.

This model assumes segregation to a single surface of a film of finite thickness. In the near surface region, the number of segments contributed by the end-modified polymer chains, pN, is related to Ω through:

$$pN = \Omega \varphi \gamma \tag{3.8}$$

where φ is the concentration of end-modified polymer in the system, and γ is the fraction of end-modified polymers which segregate to the near-surface region.

Additionally, l can be eliminated from the model equations by redefining it in terms of the system's other parameters:

$$l = pN\Lambda a^3 / L^2 \tag{3.9}$$

where $\Lambda = f/\eta + (1 - f)$.

The variables and expressions used in the model are summarized in table 3.1.

At this point in the development of the model, the two constraint equations, 3.7 and 3.8, plus the definition of l, equation 3.9, are used to define the problem in terms of two variables: η and γ. To obtain solutions, the total free energy of the system per monomer $F_{total}/k_b T \Omega$, is minimized with respect to these two variables. A FORTRAN program which computes values of F_{total} and determines the lowest point on the closed bounded region for η and γ between 0 and 1 was created and compiled. The source code for this program can be found in

Table 3.1: Parameter values used in free energy model

symbol	description
φ	concentration of end-modified polymer in homopolymer
N	total number of statistical segments in end-modified polymer [$N = N_A + N_B$]
f	A–block fraction of end-modified polymer [$= N_A / N$]
N_h	number of statistical segments in A homopolymer
α	ratio of length of end-modified polymer to homopolymer [$= N / N_h$]
η	fraction of A monomers in near-surface region contributed by the A–block of end-modified polymer
$1-\eta$	remainder of near-surface region A monomers, composed of interpenetrating homopolymer chains
Λ	fraction of monomers which segregate to comprise near-surface region [$= f/\eta + (1-f)$]
p	the total number of end-modified chains comprising the near-surface region
$\alpha p(1-\eta)/2\eta$	the total number of homopolymer chains comprising the near-surface region
γ	fraction of end-modified polymers which segregate
φ_1	concentration of end-modified monomers in volume outside the near-surface region [$= \varphi(1-\gamma)/(1-\varphi\gamma\Lambda)$]
$\varphi\gamma\Lambda$	volume fraction of system occupied by near-surface region
Ω	total number of monomers in the system
$\Omega(1-\varphi\gamma\Lambda)$	total number of A & B monomers outside the near-surface region

appendix A.

3.2 Results of Model

Three sets of parameter variations were performed utilizing the model to test its predictive capacity.

In the first set of model variations, the fraction of polymer in the near-surface region is studied as a function of the bulk concentration of end-modified material for three different matrix molecular weights. The number of segments in the end-modified additive is held constant in this series at N=65 (modeling a 7k dPS-TFE material). The matrix molecular weights were chosen as N_h=39, 386, and 3856 (modeling a 4k, 40k and 400k PS matrix, respectively). The sample thickness, h, was held constant at 750$\mathring{A}$. The results of the matrix molecular weight variations can be seen in figure 3-2. The model clearly shows that as matrix molecular weight is increased, the fraction of end-modified material near the surface increases for any given bulk concentration of end-modified material. The model also predicts that as the bulk concentration of end-modified material is increased, the fraction of end-modified material in the near-surface region increases. For the highest matrix molecular weight sampled, when the additive concentration reaches 17.5%, the near-surface region is composed entirely of end-modified material as indicated by the model.

The results in figure 3-2 can be interpreted by understanding the dependence of the free energy on molecular weight. As the molecular weight of the matrix component increases, the contribution from the mixing entropy (equations 3.5 and 3.6) to the overall free energy of the system decreases, while the energetic savings afforded by localizing the end-functional polymers near the surface (equation 3.2) increases. The fraction of end-modified chains in the near-surface region increases roughly linearly with increasing bulk concentration up to saturation, when the near-surface region is composed entirely of end-modified material.

In the second set of model variations, the fraction of polymer in the near-surface region is studied as a function of the bulk concentration of end-modified material for three different end-modified (or additive) molecular weights. The matrix in these tests was held constant at N_h=3856 (400k PS). The additive molecular weights were N=65, 650, and 3856 (7k, 70k, and 400k PS respectively). The sample thickness was held constant at 750$\mathring{A}$. The results of the additive molecular weight variations can be seen in figure 3-3. The trend of increasing end-modified fraction in the near-surface region with *decreasing* additive molecular weight can be seen for any given bulk concentration of end-modified material.

The molecular weight dependence exhibited in this set of variations can be explained by the fact that the end-functionalized tail is the same size for each molecular weight. Hence for higher molecular weights, the tail becomes less effective in anchoring the longer chains to the surface. The blends remain mixed to avoid the entropic penalty associated with inhomogeneities in the concentration profile. For equal matrix and additive molecular weights, the ratio of ϕ_s to ϕ_β is approximately 3:2.

The last model variation carried out was a test of the degree of segregation as a function of the sample's thickness, h, keeping the molecular weights constant at N=65 and N_h=386. The bulk concentration of end-modified material also remained fixed at $\phi = 0.05$. The results of the sample thickness variation study are shown in figure 3-4 for the thickness range $200\mathring{A} < h < 10,000\mathring{A}$. The overall trend is for increasing η as the sample thickness increases, but the rate of increase in η is continually slowing as h is increased. Between 0 and 1000$\mathring{A}$, η increases very rapidly, but asymptotes to approximately $\eta = 0.45$ at larger thicknesses.

The trends observed with film thickness variation can be explained as follows. For very thin films, any appreciable amount of additive segregation will significantly deplete the concentration in the interior, unfavorable from the standpoint of mixing entropy. For thicker samples the surface to volume ratio

decreases and an increase in the surface concentration is energetically favorable. The surface concentration is limited, however, by the deformation of the anchored chains, and hence η is seen to level off with increasing thickness.

3.3 Conclusions

Several predictions have been made using a phenomenological free energy model developed to study the surface segregation of end-modified chains in thin film AB/A polymer blends. Increasing segregation was observed with increasing molecular weight of the A matrix, decreasing molecular weight of the AB additive and increasing film thickness. Experiments relating to these predictions are reported on in the remainder of this thesis. It should be pointed out that computer modelling is intended here as a complement to experimentation, to give us a measure of the physical forces governing the thermodynamic behavior of these systems.

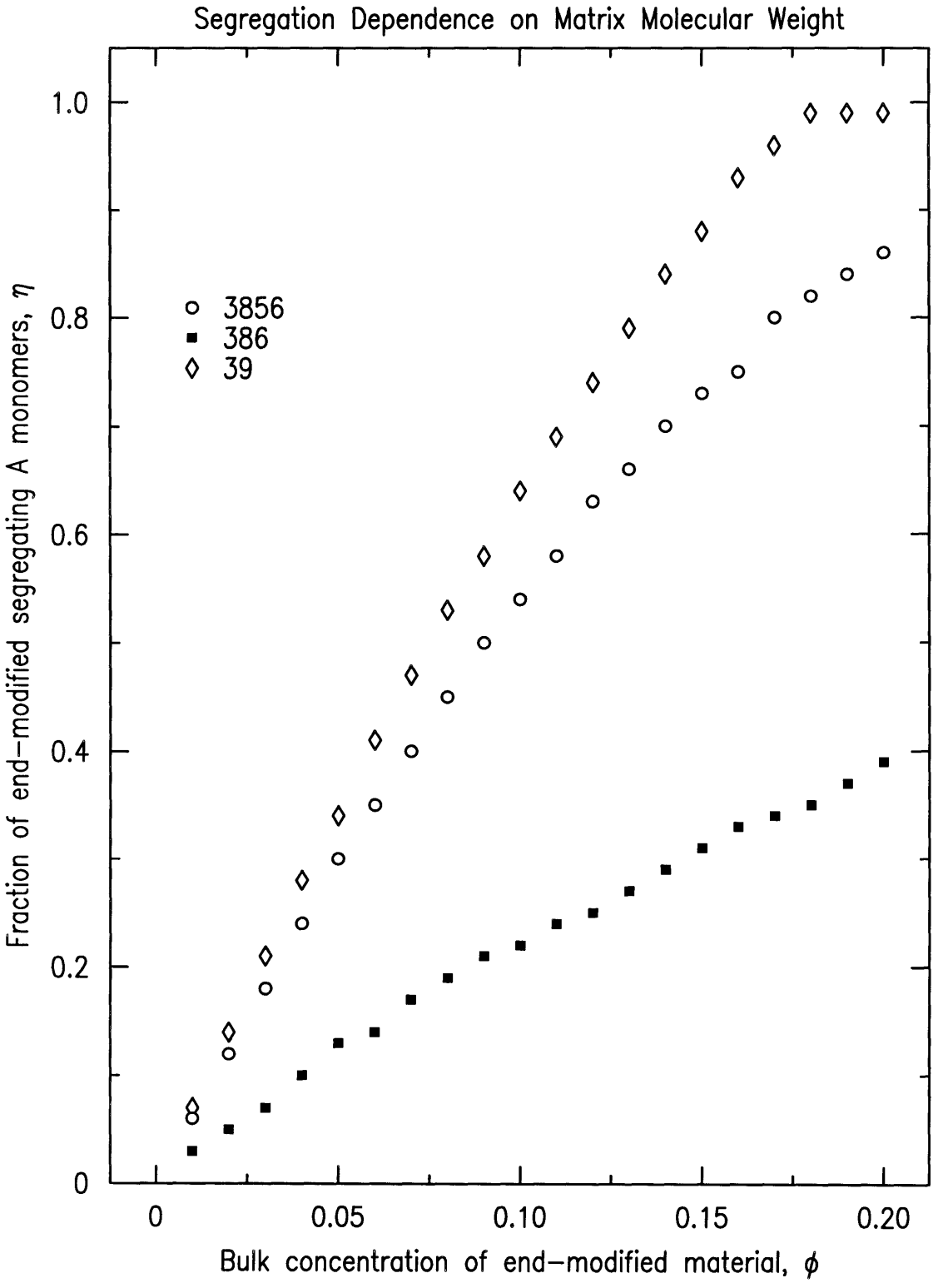

Figure 3-2: Matrix molecular weight model variations, h=750$\mathring{A}$, N=65.

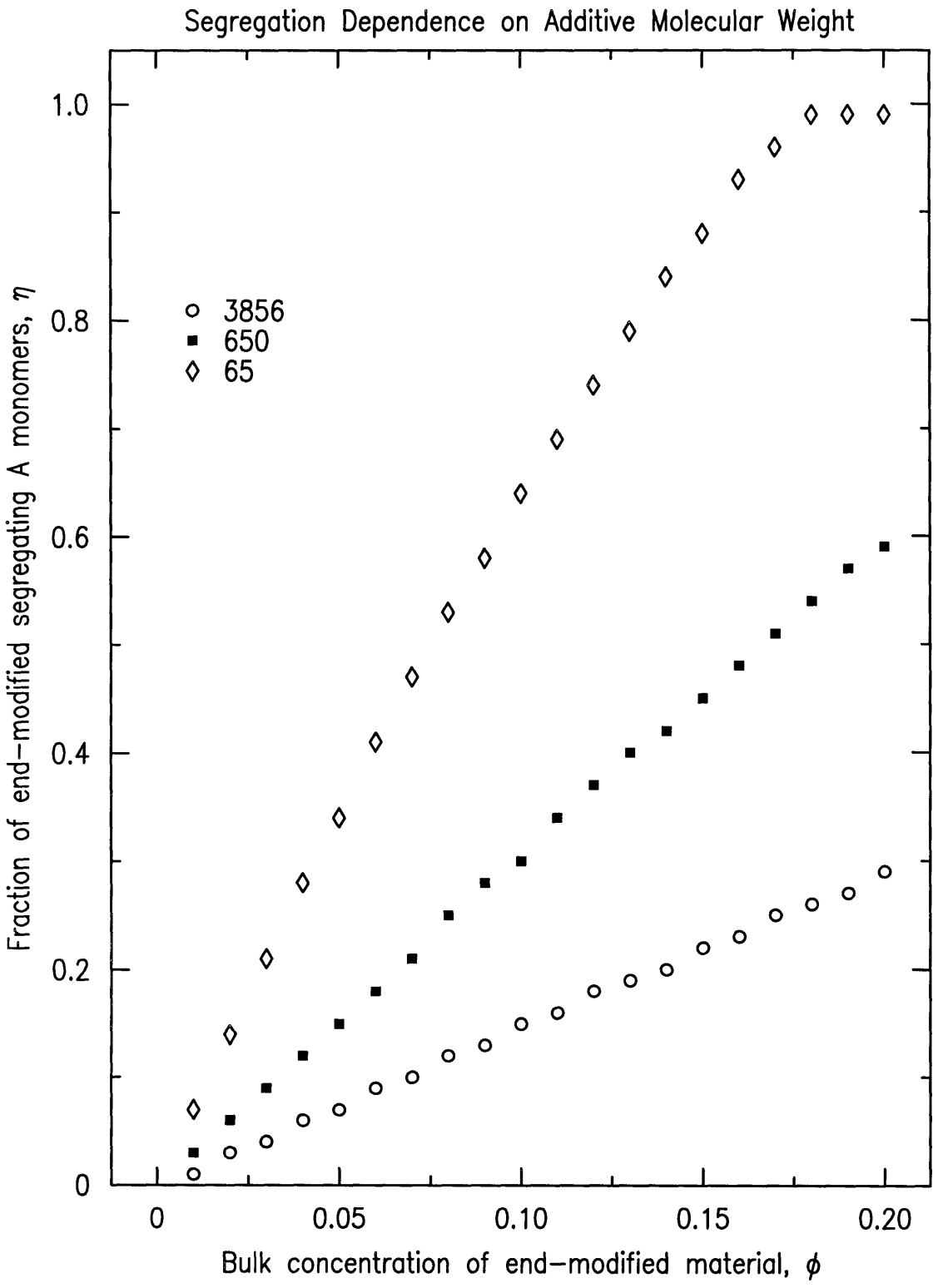

Figure 3-3: Additive molecular weight model variations, h=750$\AA$, N_h=3856.

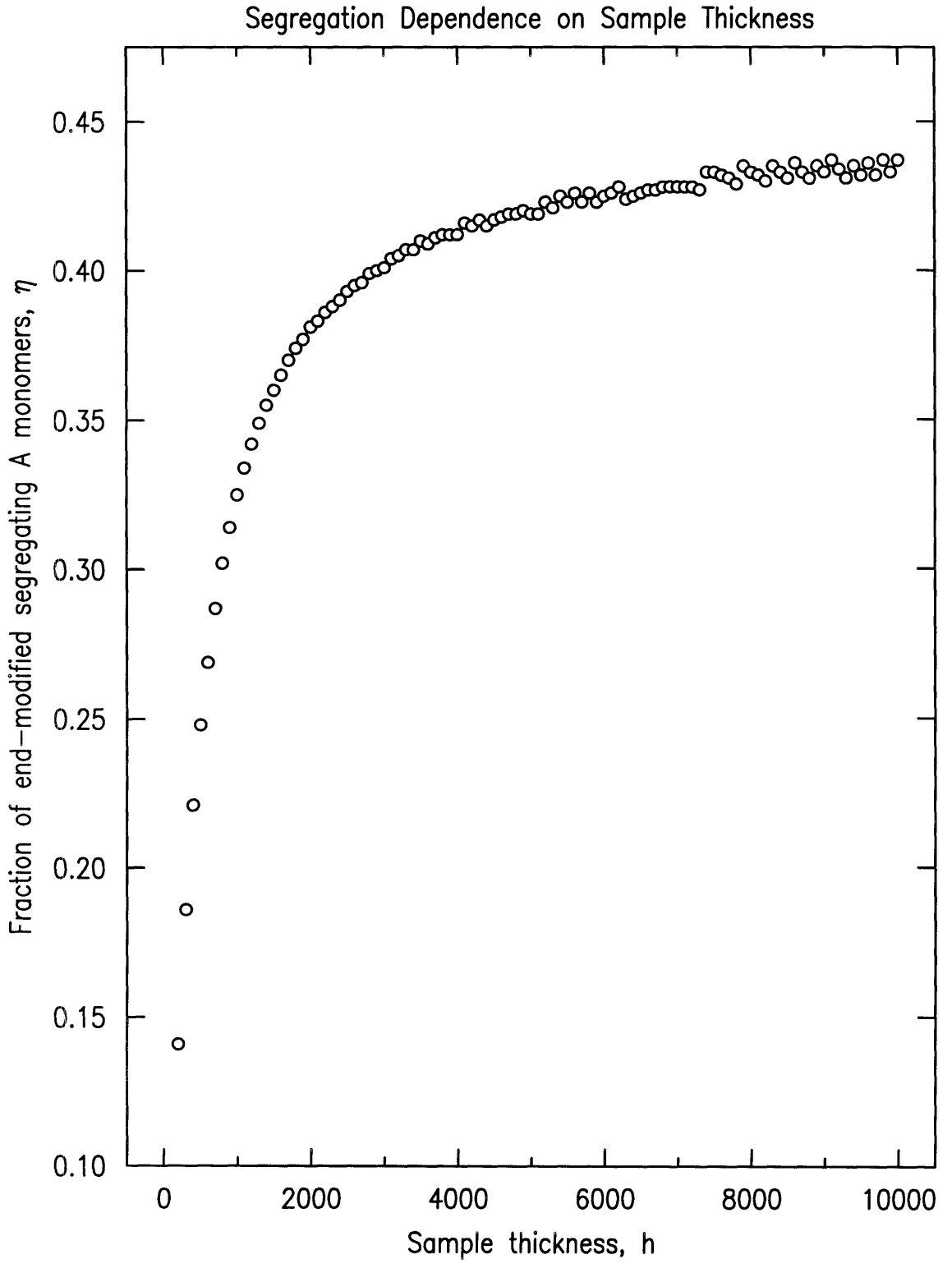

Figure 3-4: Sample thickness model variations, N=65, N_h=386, $\phi = .05$.

Chapter 4

Experimental Procedure

4.1 Synthesis of End-Functional Polystyrenes

4.1.1 General Description of Anionic Synthesis

The end-functionalized polystyrenes used for study in the present work were synthesized via a chain-growth polymerization mechanism known as anionic synthesis. The essence of this technique is the addition of electrophilic monomers, dispersed throughout a solvent, to a propagating anionic nucleophile. Perhaps the most important feature of anionic synthesis is the absence of an inherent termination process. As a result, anionic polymerization is well suited for making end-functionalized polymers; the synthesis will remain "living" until capped (or terminated) with the desired chemical end group [36]. Anionic synthesis can be ideally considered as consisting of three stages: initiation, propagation, and termination.

Organolithium compounds — such as *sec*-butyllithium — are often used as initiators in anionic polymerization of the carbon-carbon double bond [37]. These compounds are both soluble in hydrocarbon solvents and dissociate rapidly prior to the start of polymerization. Assuming initiator dissociation is instantaneous and complete, initiation proceeds as shown in figure 4-1. The styrene monomer's pendant phenyl group serves as an electron-withdrawing

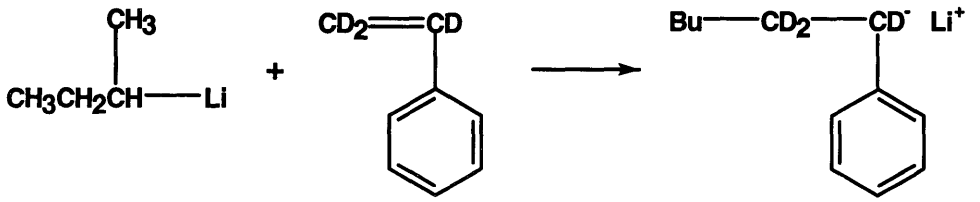

Figure 4-1: Initiation of deuterated styrene by *sec*-butyllithium

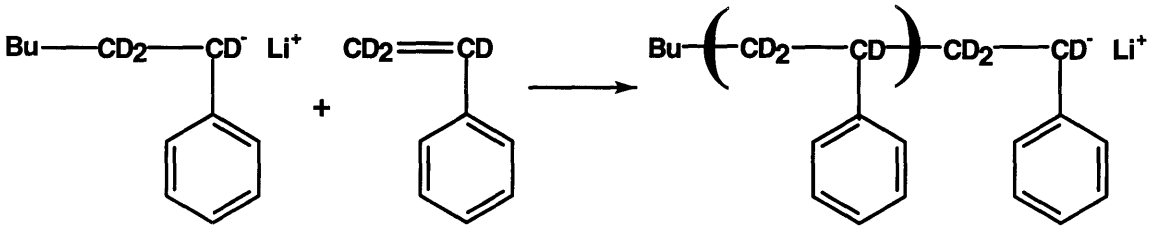

Figure 4-2: Propagation of deuterated styrene

substituent which stabilizes the carbanion. The Li^+ ion is attracted towards the negatively charged polymer and maintains charge neutrality. The extent of separation between the counterion and the propagating anion is determined by the dielectric constant of the solvent; use of a polar solvent allows a greater degree of separation between the oppositely charged ions.

Propagation, figure 4-2, is the second step of the polymerization. In an ideal treatment, this stage of the synthesis commences once all the initiation reactions have been completed. In fact, however, propagation of chains begins even as some initiator compounds are still dissociating; thus two phases of the synthesis are occurring simultaneously. In the absence of impurities, propagation will continue until the supply of monomers is depleted, at which point the propagating chains will remain viable and capable of adding more monomer if introduced to the reactor.

Termination of the synthesis is often done by reacting the living anion with a proton donor, usually an alcohol [38]. Another means of termination, however, is the addition of a compound with a leaving group, such as chlorine. In these experiments a chlorosilane is used to "cap" the propagating anionic chain, see figure 4-3.

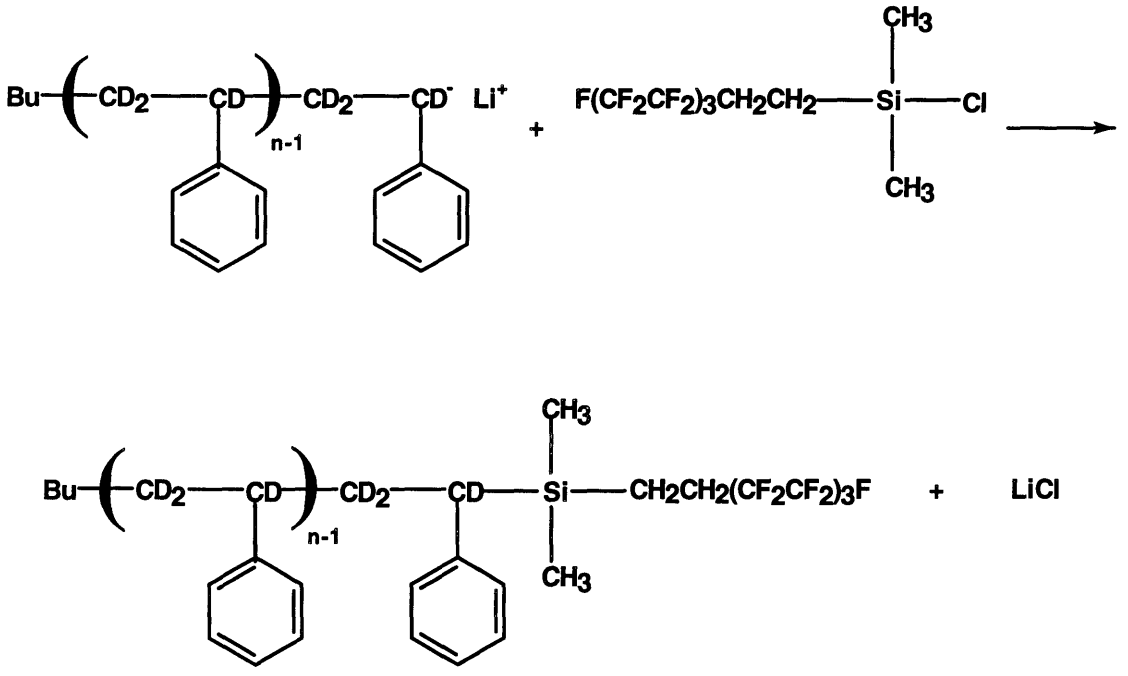

Figure 4-3: Termination of propagating deuterated styrene anion

High molecular weight polymers can be synthesized by adding small quantities of initiator to a monomer rich solvent. Assuming initiation is fast, the number-average degree of polymerization, $\overline{x}_n$, is determined by the ratio of moles of monomer consumed to moles of polymer chains produced. Given complete conversion of monomer and initiator, this is expressed simply as the initial concentration of monomer divided by the initial concentration of initiator

$$\overline{x}_n = \frac{[M]_0}{[I]_0}. \tag{4.1}$$

The polydispersity index (PDI), which measures the breadth of the molar mass distribution, is equal to the ratio of the weight-average degree of polymerization to the number-average degree of polymerization. Using $\overline{x}_n$ it can be shown [38] that the PDI is also equal to

$$\overline{M}_w/\overline{M}_n = 1 + 1/\overline{x}_n. \tag{4.2}$$

4.1.2 Synthetic Experimental Procedure

Styrene–d_8 monomer (Cambridge Isotope Laboratories) was stirred over inhibitor remover and calcium hydride (CaH_2) for one half hour to react with protic impurities. 50 mL of HPLC grade, inhibitor-free tetrahydrofuran (ER Science, OmniSolv) were added via cannula transfer to a 250 mL oven-dried, round bottom flask which served as the synthesis reactor. Prior to transfer the reactor was capped with a teflon-faced silicone septum and filled with argon to provide an inert atmosphere for the reaction. The tetrahydrofuran in the argon-filled reactor was then degassed using argon for 30 minutes to remove dissolved oxygen. Finally, after filtering excess inhibitor remover and CaH_2 from the monomer, the flask was charged with 1 mL of the cleaned styrene–d_8 monomer.

The reactor was next cooled in a dry ice/acetone bath. Thermal equilibration was reached after several minutes when the bath ceased violent boiling. Polymerization was then initiated by the addition of a 1.3M solution of *sec*-butyllithium in cyclohexane (Aldrich Chemical) to the reactor with syringe via septum. Various quantities of *sec*-butyllithium solution, from 0.01 mL to 1.2 mL, were introduced in each run to obtain a range of molar masses. The resulting solution turned yellow-orange upon initiation, indicating the presence of carbanions, and was stirred for 3 hours to ensure complete reaction. The polymerization was functionally terminated with the addition of an excess of (tridecafluoro-1,1,2,2-tetrahydrooctyl)-1-dimethylchlorosilane (Petrarch Silanes and Silicones) via syringe. The solution immediately turned clear.

Once terminated, the solution was brought to room temperature and stirred for 15 minutes, during which time it became cloudy due to the precipitation of lithium chloride. The polymer solution was then precipitated into a 15-fold excess of methanol (ER Science, OmniSolv) and vacuum filtered. Soxhlet extraction was performed for 12 hours using methanol to remove any impurities. The resulting product was then dried for 12 hours under ambient pressure with

slight heating.

4.1.3 Polymer Characterization

Gel Permeation Chromatography

Gel permeation chromatography (GPC) was performed on a Waters Associates GPCII Gel Permeation Chromatograph to determine molar mass distributions for the polymers synthesized. Details concerning this technique can be found in [38]. Chromatograms for the end-functionalized polystyrenes synthesized in section 4.1.2 are displayed in appendix B. The method used for calculating M_n and M_w from the chromatograms is explained in [39]. Table 4.1 provides a summary of expected and measured results concerning molar masses and molecular weight distributions.

Table 4.1: GPC molar mass results

Sample	$\frac{[M]_0}{[I]_0}$	expected M_n	expected PDI	measured M_n	measured M_w	measured PDI
1	5.49	1175	1.18	4013	4920	1.23
2	27.45	3636	1.04	6343	7730	1.22
3	34.3	4403	1.03	7230	9144	1.26
4	137	15940	1.01	9293	13295	1.43

Differential Scanning Calorimetry

Differential scanning calorimetry (DSC) was conducted on a Perkin-Elmer DSC 7 to measure the glass transition temperatures of the synthesis products. DSC is a thermal analysis technique which measures the difference in power required to keep a sample and reference chamber heating at the same rate. More information on this technique can be found in [40]. T_g values for both heating and cooling curves, scanning at a rate of plus or minus 20°C per minute respectively, are given in tables 4.2 and 4.3. (This is the first time T_g

Table 4.2: DSC T_g measurement results

Description	$T_g^h(°C)$	$T_g^c(°C)$
4.0k dPS-TFE	77.58	76.06
6.3k dPS-TFE	89.41	84.23
7.2k dPS-TFE	93.24	87.45
9.3k dPS-TFE	97.20	90.57

Table 4.3: DSC T_g measurement results

Description*	$T_g^h(°C)$	$T_g^c(°C)$
6.3k PS-TFE	87.29	83.23
7.4k PS-TFE	94.19	88.65
12.7k PS-TFE	94.28	88.76
23k PS-TFE	99.61	94.43
39k PS-TFE	101.87	94.92
59k PS-TFE	102.09	95.03
94k PS-TFE	103.39	97.09

* synthesized by D. Lee [41]

values are being reported for the samples listed in table 4.3. Details concerning the synthesis of these polymers can be found in [41].)

DSC results are plotted in figure 4-4 as T_g versus $1/M_n$ for heating and cooling curves. Bulk T_g's, as mentioned in section 2.2, scale inversely with molecular weight — see equation 2.3. For polystyrene homopolymer (PS) the limiting T_g value (*i.e.* $T_{g,\infty}$) is known to be 373K with $k_b = 114,400$ [27]. Regression analysis of the DSC data reveals that limiting T_g values for the end-labelled polymers are in excellent agreement with PS homopolymer — *viz.* $T_{g,\infty}^c = 370.6$K and $T_{g,\infty}^h = 377.8$K — with slopes (*i.e.* k_b values) for both heating and cooling curves less than PS — 99,000 and 82,000 respectively. These findings indicate that the thermal behavior of the end-functionalized polymers is identical with PS for high molecular weights where the contributions from chain

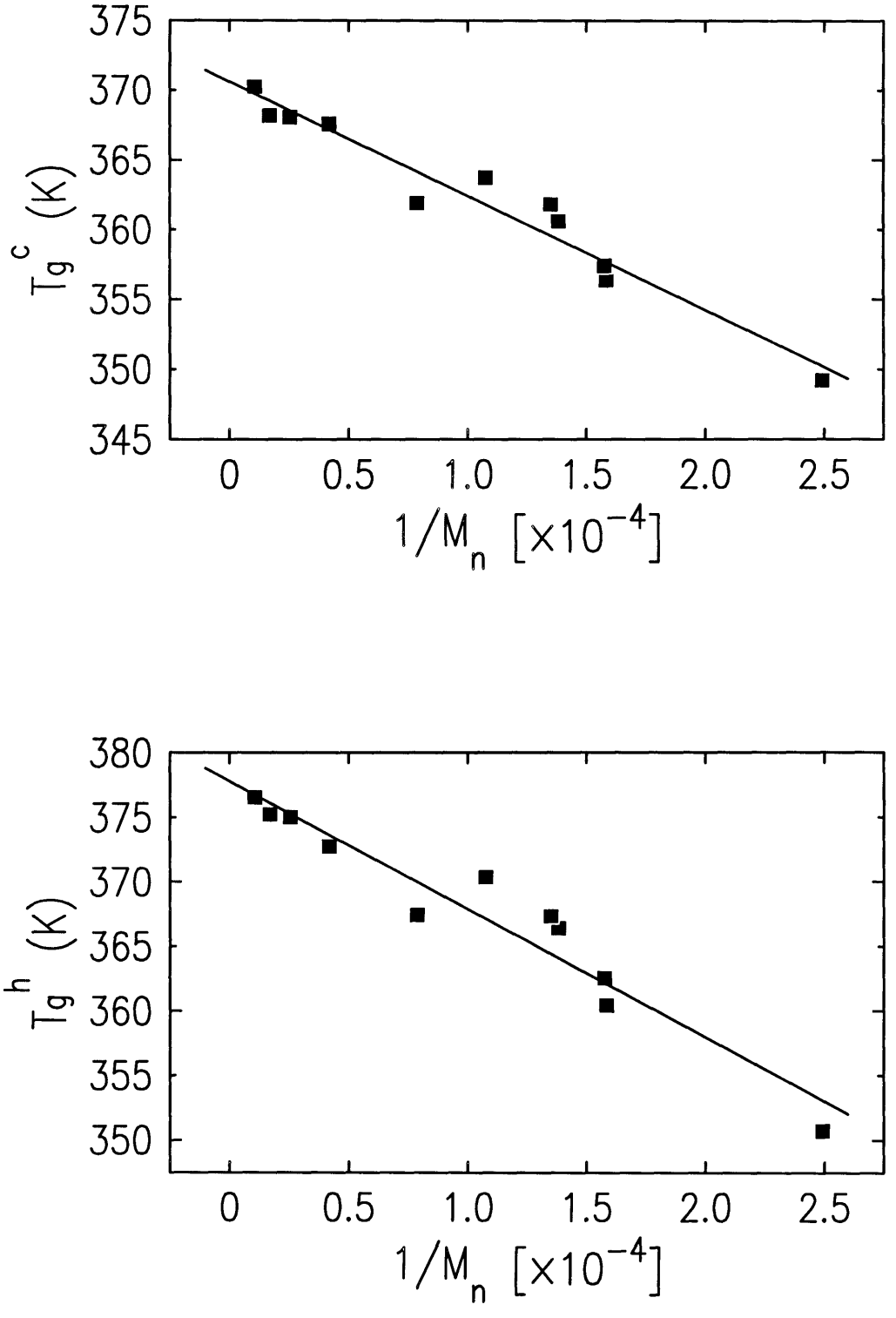

Figure 4-4: T_g dependence on M_n for end functionalized PS and dPS polymers.

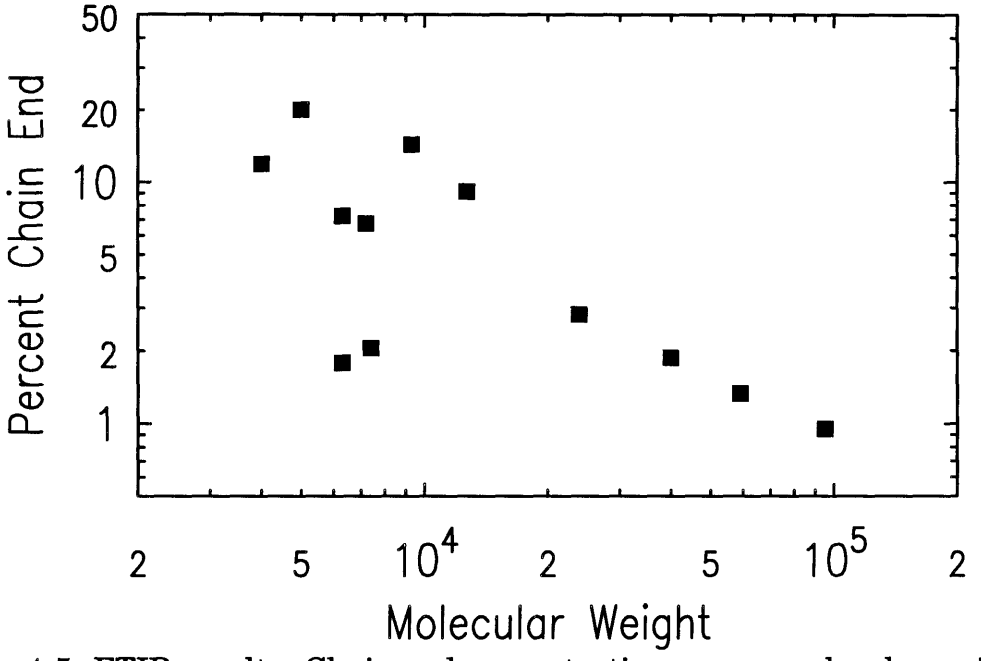

Figure 4-5: FTIR results: Chain end concentration versus molecular weight.

ends are negligible. The more gradual slopes indicate that at lower molecular weights the functionalized chain end is altering the thermal properties.

Fourier Transform Infrared Spectroscopy

Fourier transform infrared spectroscopy (FTIR) was performed on a Nicolet 510P FT-IR Spectrometer to determine the bulk concentration of functionalized chain ends for the polymers synthesized in section 4.1.2 as well as the polymers from [41]. Details concerning this technique can be found in [42]. Bulk concentrations of chain ends were measured by examining the relative strengths of two signals from the FTIR transmission spectra. To characterize the functionalized chain ends, the signal strength of the aliphatic $Si\text{-}CH_3$ group at 1250 cm^{-1} was used. Bulk concentrations of the end-functionalized polymers' styrene component were measured from the signal strengths of the asymmetric stretching modes of the styrene's phenyl group; in protonated styrene these signals fall near 1450 and 1490 cm^{-1}, while in deuterated styrene they are shifted to lower frequencies at 1330 and 1370 cm^{-1}.

Nuclear Magnetic Resonance

Nuclear magnetic resonance (NMR) was performed on a Bruker WM250 to further quantify the bulk concentration of functionalized chain ends. Information concerning this analytical technique can be found in [43, 38]. NMR is based on the fact that when a nucleus with non-zero spin is placed in a magnetic field there is a splitting of the quantized magnetic energy levels, or Zeeman levels. Transitions between energy levels can be induced by supplying a resonant radio frequency magnetic field in addition to a static magnetic field to split the degenerate states. Protons, which have a spin of 1/2, will resonate at slightly different frequencies depending on their chemical binding positions within a molecule, and these shifts can in turn be used to characterize the molecule's chemical composition. NMR spectra were taken on the 6.3k PS-TFE and 7.2k dPS-TFE samples synthesized in house, and on a 500 PS-TFE sample supplied by Professor J. DeSimone at the University of North Carolina. The NMR spectra from these studies are presented in appendix C.

4.2 Investigative Techniques

4.2.1 X-ray Photoelectron Spectroscopy

X-ray photoelectron spectroscopy (XPS) measurements were performed on a Perkin Elmer 5000 Series ESCA System to determine the surface concentration of fluorinated chain ends. Extensive details regarding this technique can be found in [44]. XPS is generally used to measure the chemical composition of samples within a region about 2 nm from the sample's surface. This technique involves subjecting samples to hard x-rays, with wavelengths of $\lambda \approx 10\mathring{A}$, and recording the kinetic energies of the ejected core, or photo-electrons. The energy levels of these electrons are characteristic of the atomic species from which they originated, thus revealing uniquely the identity of the material. The low conductivity of polymer samples creates immobile positive hole charges, which

are left behind by the ejected electrons. This may create an electric charge potential resulting in the loss of some kinetic energy of the electrons [45], thereby complicating the experimental analysis.

4.2.2 Contact Angle Measurements

Contact angle measurements were taken on a VCA2000 Video Contact Angle System by ASE, Inc. This method of measuring surface tension is based on the Young equation for contact-angle equilibrium [46]. For a liquid drop on an ideal substrate, the relation between the contact angle and the various interfacial tension components is given by

$$cos\theta_e = \frac{\gamma_{SV} - \gamma_{SL}}{\gamma_{LV}} \tag{4.3}$$

where L, V and S stand for liquid, vapor, and solid respectively, and θ_e is the equilibrium contact angle. The interfacial tension forces are represented schematically in figure 4-6. Water was the testing liquid used , with γ_{LV}=72.8 dyne/cm.

4.2.3 Neutron Reflectivity

Neutron reflectivity (NR) measurements were performed on the Grazing Angle Neutron Spectrometer (GANS) at Missouri University's Research Reactor Facility (MURR) in Columbia, Missouri in collaboration with Dr. John Ankner. Extensive details concerning this technique can be found in [47]; a brief discussion with information pertinent to the present work is given here. Specular reflection of neutrons at a surface or interface depends on the difference in the refractive indices of the two adjacent media. The refractive index for neutrons is given by

$$n = 1 - \frac{1}{2\pi}\lambda^2\frac{b}{V} \tag{4.4}$$

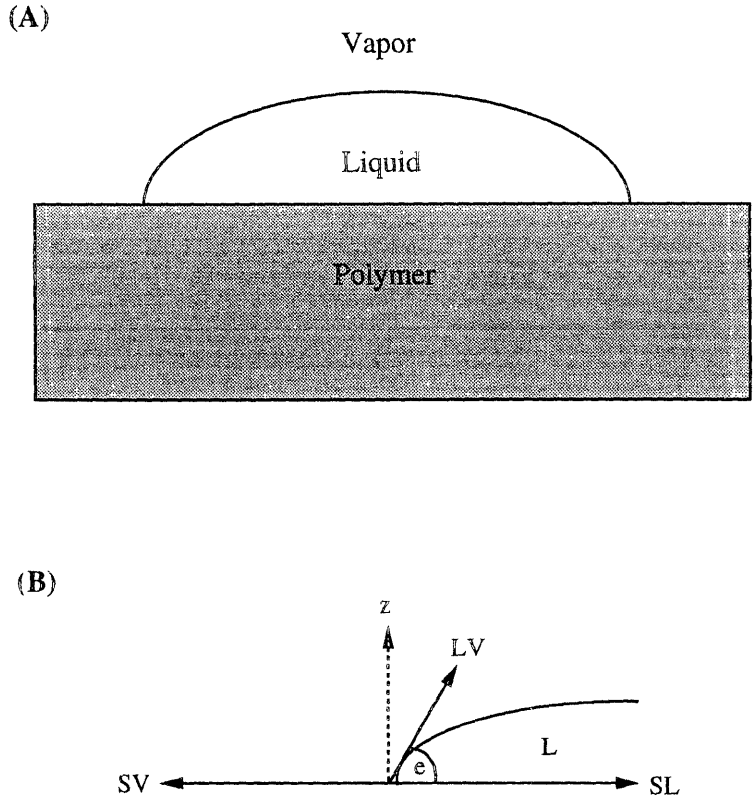

Figure 4-6: (A) Example of droplet used for contact angle measurements. (B) Schematic illustration of force balance in contact angle measurements.

where λ is the neutron wavelength, and b/V is the material's scattering length density [48].

The NR technique involves measuring the reflected beam intensity as a function of the normal component of the neutron's momentum vector in a vacuum $k_{z,0} = \frac{2\pi}{\lambda}\sin\theta$, where θ is the incident angle between the neutron beam and the specimen. In a homogeneous specimen the neutron momentum normal to the surface is written as [49]:

$$k_{z,1} = (k_{z,0}^2 - 4\pi(b/V)_1)^{1/2} \tag{4.5}$$

where $(b/V)_1$ is the specimen's scattering length density. For $k_{z,0}^2 < 4\pi(b/V)_1$, $k_{z,1}$ is imaginary; the neutrons propagate into the material only as an evanescent wave, giving rise to total external reflection. For $k_{z,0}^2 > 4\pi(b/V)_1$ neutrons are able to penetrate into the material and the intensity of the reflected wave's amplitude is recorded as the reflectivity, R. The reflectivity for the simplest case of a sharp interface between a sample and air, shown schematically in figure 4-7, is given by the Fresnel expression [50]

$$R = |r_{0,1}|^2 = (\frac{k_{z,0} - k_{z,1}}{k_{z,0} + k_{z,1}})^2 \tag{4.6}$$

which has a limiting form at high $k_{z,0}$ of $R \approx \pi^2(b/V)^2 k^{-4}$.

Reflectivity calculations can quickly be extended to the multilayer case — where a stack of thin slabs is present — by the following recursive scheme. The reflectance of a sharp individual interface between layers i and $i-1$ may be denoted $r_{i-1,i}$ and again is given by the Fresnel expression:

$$r_{i-1,i} = \frac{k_{i-1} - k_i}{k_{i-1} + k_i}.$$

If $r_{i-2,i}$ is the combined reflectance of the interface between the substrate and

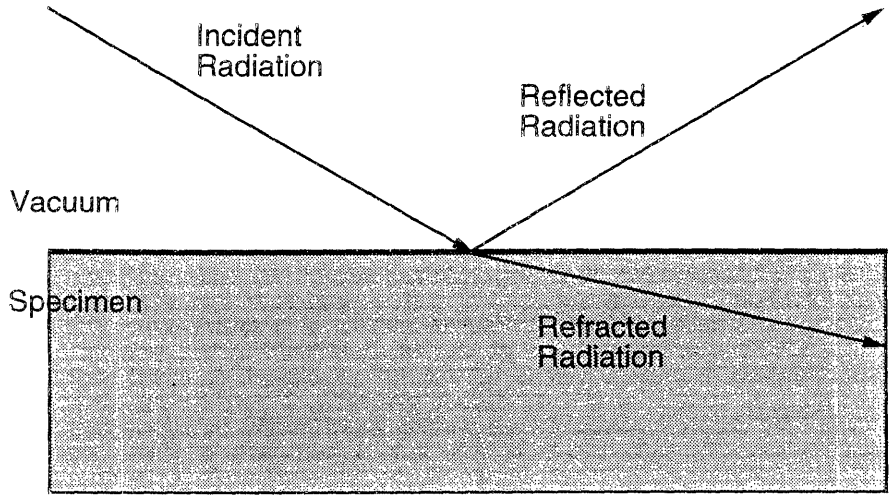

Figure 4-7: Simple geometry for neutron reflectivity

layer $i-1$, and layers $i-1$ and $i-2$, then this can be written as

$$r_{i-2,i} = \frac{r_{i-2,i-1} + r_{i-1,i}\exp(2ik_{i-1}d_{i-1})}{1 + r_{i-2,i-1}r_{i-1,i}\exp(2ik_{i-1}d_{i-1})}$$

by imposing continuity conditions on the wavefunction and its derivative at the layer boundaries. This algorithm can be repeated indefinitely until the top surface is reached, and constitutes the basis of a computer program used to model reflectivity profiles. By approximating the profile of a real, continuous sample with a series of slabs, the reflectivity may be calculated to any degree of accuracy required for a given k range.

Scattering length density values for materials used in these experiments are presented in table 4.4.

4.3 Sample Preparation

The end-functionalized polymers synthesized as described in section 4.1.2, and in references [41] and [51], as well as varying molecular weight polystyrene standards (Aldrich Chemical Company) were made into samples by first dissolv-

Table 4.4: Material constants used in reflectivity analysis.

material	density (g/cm^3)	(b/V) ($\times 10^{-6} \AA^{-2}$)
sec-Butl	0.769	-0.01
TFE	1.05	2.27
PS	1.0	1.43
dPS	1.08	6.1
Si	2.32	2.084
SiO_2	2.20	3.05

ing these polymers in toluene (Mallinckrodt AR). The polymer solutions were filtered using Millipore GVHP013 0.22μm filters to remove large impurities. Two categories of samples were then prepared: thin films of end-functionalized polymers for XPS, NR and contact angle measurements; and thin films of AB/A blends with end-functional PS and PS homopolymer for NR and contact angle measurements.

Polished silicon wafers (Exsil) — for NR, 10 cm in diameter; for XPS and contact angle measurements, approximately 1 cm^2 wafer sections — were immersed for a 24 hour period in chromic-sulfuric acid solution (Fisher Chemicals) to remove any hydrocarbon impurities. Upon removal, the wafers were rinsed with deionized water (18.2 MΩ-cm), and coated with 1,1,1,3,3,3 hexamethyldisilazane (Aldrich Chemical) for surface treatment [52]. Treating the silicon with this modification agent renders the surface very hydrophobic and inhibits dewetting of the polymer solution upon spin casting. After approximately one hour the wafers were again rinsed with deionized water, then immersed in a deionized water bath for 20 minutes. This rinsing procedure was repeated several times to remove excess disilazane, leaving a monolayer coating.

The sub-micron film thicknesses desired for samples was obtained by spin coating the filtered polymer solutions. A description of this technique can be found in [53]. Briefly, by varying the spin speed and concentration of the polymer solutions, sample thicknesses ranging from 100$\AA$ to 1500$\AA$ were obtained.

Thickness measurements were made for selected samples using a Gaertner Scientific Corporation L3W26C.488.830 Ellipsometer; additionally, thickness measurements were checked via NR. The final step in sample preparation was annealing, for which a NAPCO E Series Model 5831 Vacuum Oven was used. An evacuated oven at temperatures of 110°C and 140°C was used over time periods ranging from 15 minutes to several hours to allow the spin-coated samples to attain their equilibrium configurations and to evaporate off any remaining solvent.

Chapter 5

Results and Discussion

5.1 Chain End Segregation

5.1.1 Scaling Relations

Figure 5-1 displays the FTIR data from section 4.1.3. As mentioned previously, the concentration of chain ends in the bulk scales as N^{-1}. From the regression analysis performed on all of the FTIR data, the scaling factor was experimentally determined to be -0.72. Most of the FTIR data fall within a fairly narrow linear regime with the exception of two data points representing the 6.3k dPS-TFE and 7.4k PS-TFE samples. The FTIR data for these samples indicates that the bulk concentration of functionalized chain ends is exceptionally small.

To resolve the apparent anomaly presented by the FTIR data, an examination of the GPC data for the two samples was undertaken. GPC data for the 6.3k dPS-TFE sample is provided in appendix B, figure B-2; GPC data for the 7.4k PS-TFE sample can be found in [41]. Both chromatographs reveal a secondary molecular weight distribution, or "shoulder", on the high side of the sample's primary molecular weight distribution. The portion of the total synthesis product attributable to the shoulder was determined from the chromatographs to be 14% and 16% respectively.

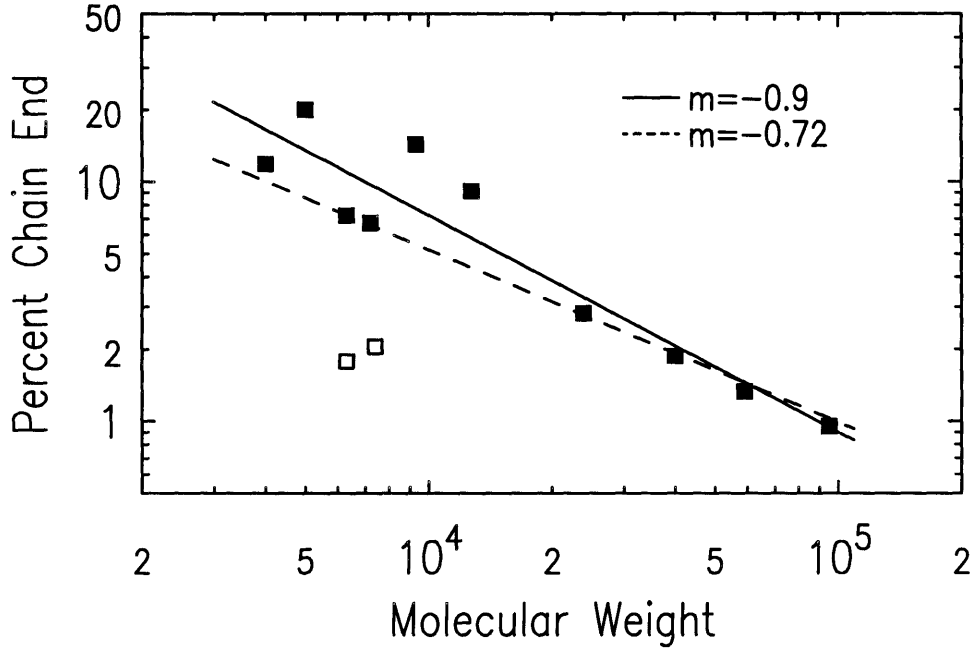

Figure 5-1: Scaling factor determination for bulk chain end concentration.

Figure 5-1 further displays a slope of m=-0.9 as the scaling factor when the FTIR data is analyzed without the 6.3k dPS-TFE and the 7.4k PS-TFE data points. Using the regression line excluding the two data points (m=-0.9) as a reference, the fraction of silane-terminated 6.3k dPS-TFE and 7.4k PS-TFE polymer chains based on the actual data points is estimated to be 16% and 20% respectively. These values are in relative agreement with the GPC data, and taken together imply that only modest fractions of the total 6.3k dPS-TFE and 7.4k PS-TFE polymers synthesized were terminated successfully.

The scaling relation for the bulk concentration of chain ends determined via FTIR is in good agreement with the expected molecular weight dependence. As an absolute measure of chain end concentration however, the FTIR measurements consistently overestimate the successfully terminated sample fraction; for example, the concentration of end-modified tails as measured by FTIR for the 6.3k PS-TFE sample is 7.2% compared with the calculated value of 1.8% for a fully terminated system. The NMR measurements taken on selected samples serve as an independent determination of the extent of successful termination. Figure C-2 displays the NMR spectrum for the 6.3k PS-TFE sample along with

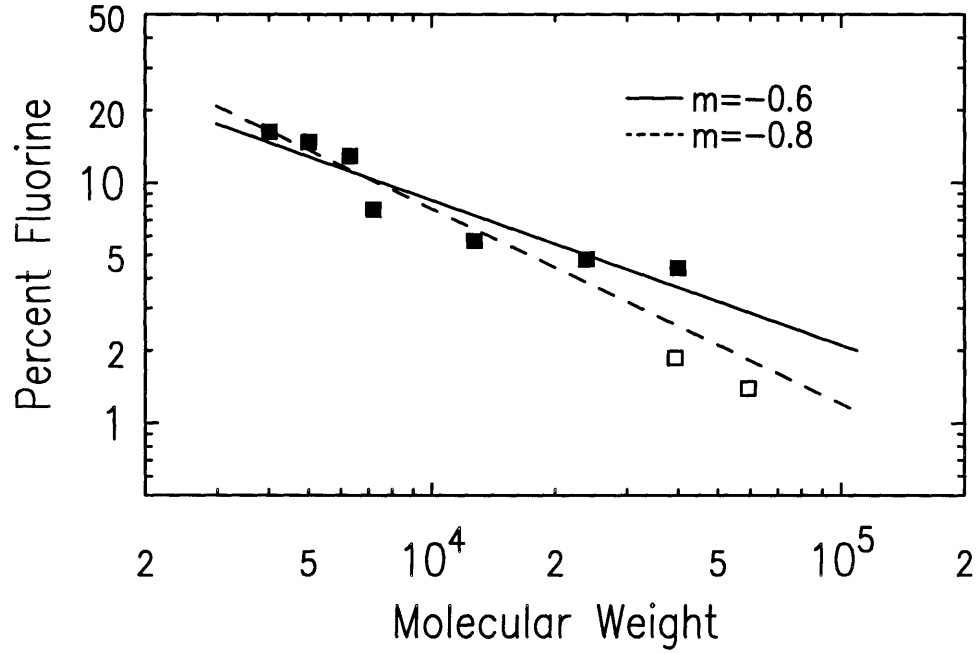

Figure 5-2: XPS determination of the surface chain end concentration.

our interpretation of which protons correspond to each of the spectral features. Based on this analysis and the GPC data from [41] it was determined that approximately 90% of the 6.3k PS-TFE sample was functionally terminated with the TFE end group.

Figure 5-2 shows the results from the XPS analysis described in section 4.2.1. Recall from equation 2.5 that the concentration of chain ends at the surface for a system in the intermediate segregation regime is expected to scale as $N^{-1/2}$. The least-squares fit to all of the data — represented by the dashed line — gives a scaling factor of m=-0.81. The large disparity between the 39k PS-TFE and 40k PS-TFE data points can be reconciled on two accounts. First, GPC data for the 39k PS-TFE sample in [41] distinctively showed a higher molecular weight secondary distribution amounting to 8% of the total for that sample; second, the FTIR data for the 39k PS-TFE sample showed a complete absence of the Si-CH_3 signal at 1250 cm^{-1} characteristic of the functionalized end-group. Based on these criteria, the 39k PS-TFE data point was discarded.

The data point for the highest molecular weight in figure 5-2, 59k PS-TFE, appeared to be well below the expected surface concentration of chain-ends for

a molecular weight of that size. The XPS measurements were taken with the samples tilted at a 65° angle from the normal to achieve the greatest possible surface sensitivity to the x-ray beam. The XPS data had to be taken with only a minimal exposure of each sample to the beam due to the issue of sample degradation [54]. Counting statistics for the 59k PS-TFE sample were therefore very poor. Additionally, XPS measurements on the 95k PS-TFE sample showed no trace of fluorine. Discarding these measurements, and performing regression analysis of the remaining seven data points, results in a slope, or scaling factor, of m=-0.6, compared to m=-0.5 predicted.

5.1.2 Reflectivity Studies

Neutron reflectivity (NR) measurements were taken on thin films of the dPS-TFE samples. The film thicknesses desired for these studies were on the order of a few times the radius of gyration for each sample. This thickness range was chosen to localize all chain ends at either the film's surface or substrate, leaving the interior of the film free of all chain ends. These films were prepared as described in section 4.3 on silazane-treated Si wafers and annealed for 10 to 15 minutes at 110°C.

Figure 5-3a shows the reflectivity profile for the 7k dPS-TFE sample film. The inset displays the scattering length density, or b/V profile, for the best fit curve to the data — shown as a solid line superimposed on the reflectivity profile. The best fit curve was achieved by utilizing a computer program to minimize the χ^2, or "goodness of fit" parameter, within the physical constraints set by the model. Figure 5-3b shows the distribution of chain ends throughout the film. The distribution is obtained by decomposing the b/V profile into the components which constitute the system in the following manner:

$$\frac{b}{V}_{TOT}(z) = \frac{b}{V}_1 \phi_1(z) + \frac{b}{V}_2 \phi_2(z) \tag{5.1}$$

where 1 represents the dPS backbone, and 2 represents the *combined* TFE/*sec-*

Butyl constituents, ϕ_i is the volume fraction of component i, and z is the depth normal to the surface.

For the 7k sample the bulk volume fraction of chain ends — including both the fluorocarbon tails and initiator fragments, to which the neutrons are sensitive — equals 7.7% of the total segment population. Integrating the volume fraction of chain ends over the film's thickness, the NR results indicate the film is composed of 10.7% chain ends. Potential sources for this 3.0% discrepancy include: 1) incorrectly estimating the combined b/V of the TFE and *sec*-Butyl ends (see table 4.4); 2) neglecting the substrate's surface treatment, which leaves a low b/V molecular monolayer on the oxide surface; and 3) low sensitivity of NR to the "shoulders" at $10\mathring{A}$ and $90\mathring{A}$ in the model profile.

It is also useful to examine the agreement between an NR profile generated by a model assuming a homogeneous distribution of chain ends throughout the film, and the actual reflectivity data for the film. Such a test provides an indication of how sensitive NR is to chain end segregation. Figure 5-4 displays the reflectivity profile generated by assuming a film $91\mathring{A}$ thick with a b/V value equal to the integrated b/V determined from the best fit. To obtain this profile the b/V was fixed and the program was allowed to adjust the total film thickness, with a characteristic roughness of $3\mathring{A}$ included at the surface and interface. A simple qualitative comparison shows the agreement between the model and data in figure 5-3 is much better than the homogeneous distribution of chain ends in figure 5-4, indicating that reflectivity is indeed sensitive to the segregation of chain ends in these polymer films.

5.1.3 Contact Angle Measurements

Contact angle measurements were made on thin films of the end-functionalized polymers and on unmodified polystyrene thin films. Molecular weights ranged from 4k to 90k for each series. The purpose of these measurements was to observe what effect, if any, the fluorocarbon end group has on altering the

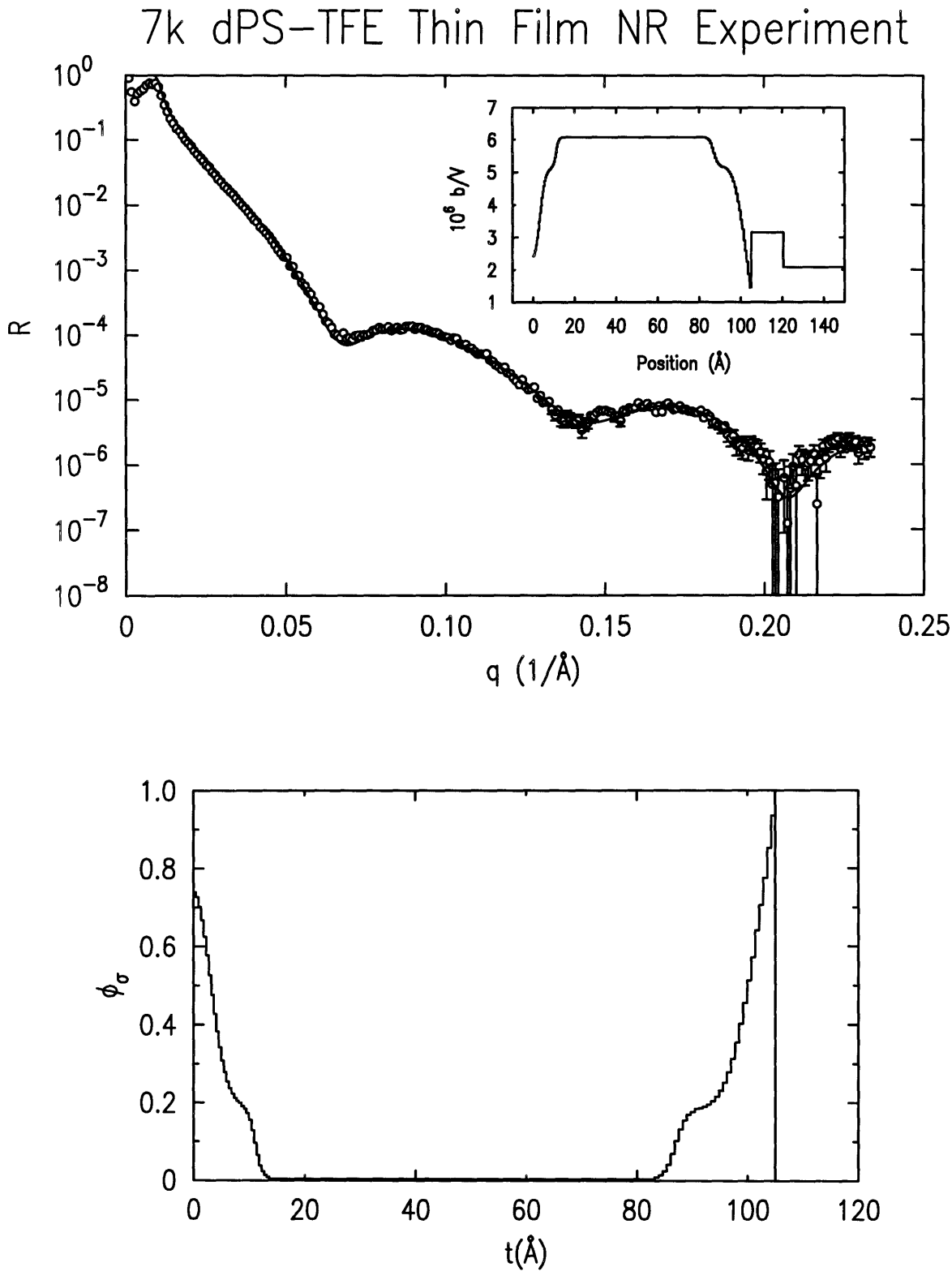

Figure 5-3: Thin film NR studies on 7k dPS-TFE sample

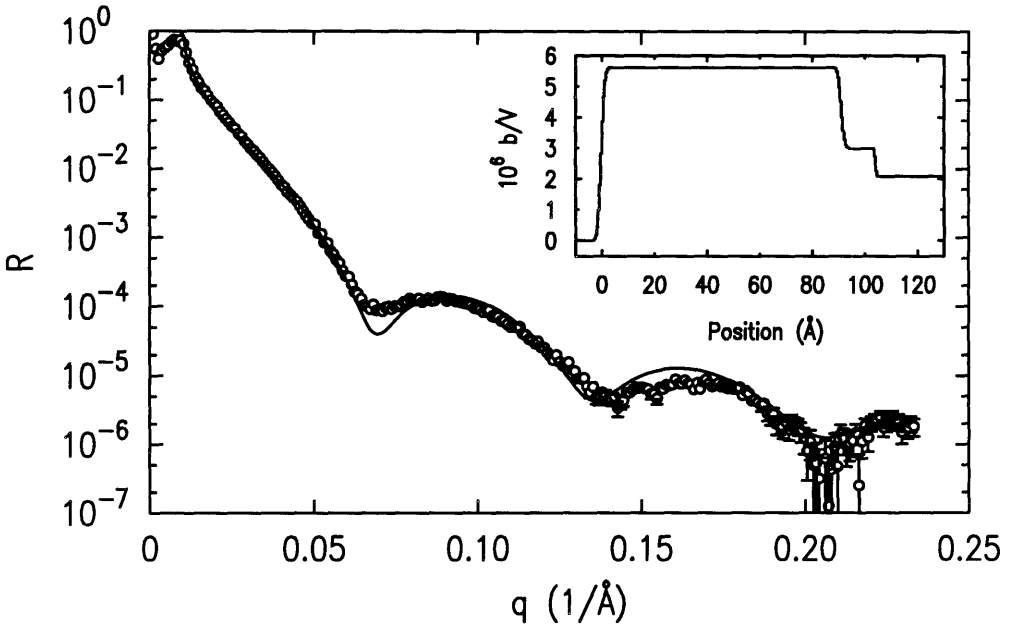

Figure 5-4: 7k dPS-TFE thin film assuming no chain end segregation

surface tension of the thin films. Comparing the end-functionalized polymers to polystyrenes of equal molecular weight isolates the effect of the chain end on the surface tension.

These measurements were made as advancing angle measurements, meaning the surface is advanced into contact with the liquid and the measurement is taken immediately after. Water was the test liquid used for these experiments. Films were annealed for 3 hours at 160°C. Error in these measurements can be attributed to surface roughness, and to inhomogeneities in the surface composition.

The contact angles measured as a function of molecular weight are shown in figure 5-5. A larger measured angle indicates a surface with a lower energy or, specifically, one which is more hydrophobic. For reference, contact angle measurements taken on a polytetrafluoroethylene thin film sample were recorded at $116.2^{o} \pm 1.14^{o}$, in outstanding agreement with previously published data [55]. From the data it can be observed that for molecular weights below 25k the silane group has a measurable effect on lowering the surface energy. Above 25k, contact angle measurements cannot distinguish between the end-functionalized

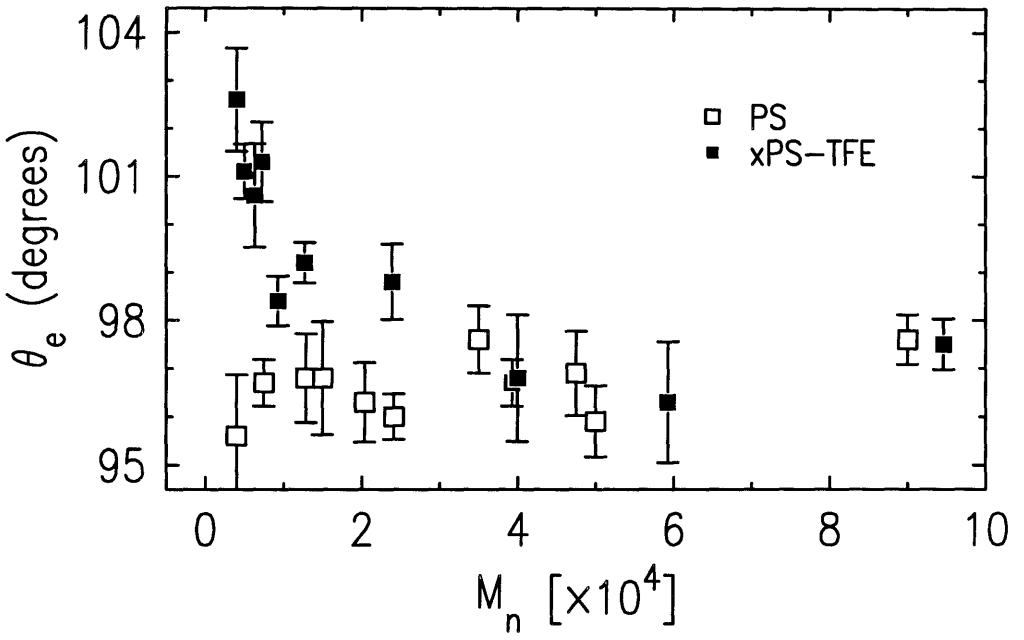

Figure 5-5: Equilibrium contact angles as a function of molecular weight.

and unmodified polystyrene. The PS samples showed little dependence on molecular weight throughout the range sampled.

Photographs of the 4k PS and 4k PS-TFE measurements are shown in figures 5-6 and 5-7 (note that these photographs have been scaled for formatting purposes). Comparing these low molecular weight systems, a pronounced difference in contact angles is observed. Based on the scaling relation from equation 2.5 the surface concentration, ϕ_s, of chain ends for a 4k PS sample is expected to be 32%. The surface concentration of TFE tails can be calculated from:

$$\theta_{e,measured} = \theta_{e,PTFE} * \phi_{TFE,\sigma} + \theta_{e,PS} * (1 - \phi_{TFE,\sigma}) \tag{5.2}$$

Using the contact angle data from the 4k PS, 4k PS-TFE, and PTFE samples, $\phi_{TFE,\sigma}$ =33%, after equation 5.2.

This result is in excellent agreement with the scaling relation, assuming the three TFE chain end segments — see figure 4-3 — can be effectively counted as two PS segments due to size differences. Furthermore, the NR data from figure 5-3 indicates a surface chain end coverage of approximately 75%, ac-

counting for both the TFE and initiator fragment ends. This result is in good agreement with the independent contact angle measurements which suggest a total surface concentration from both ends of 66%.

Photographs of the 90k PS and 94k PS-TFE contact angle measurements are shown in figures 5-8 and 5-9. For a 90k PS sample, the surface coverage of chain ends is expected to equal 7%. At this high molecular weight, contact angle measurements showed no enhancement due to the TFE ends, as recorded in figure 5-5.

5.2 End Functional Polymer Blends

5.2.1 Reflectivity Studies

Having observed chain end segregation in neat samples of end-modified polymers, the next set of experiments was intended to study the usage of end-modified polymers to control surface properties in mixtures with commodity plastics. For this purpose AB/A blend systems, consisting of end-modified polystyrene in a polystyrene matrix, were studied via NR as a function of concentration of end-functionalized polymer and as a function of the isotopic labelling of each component. A series of control experiments was also performed to determine the role entropy plays in the AB/A blends, and to separate the dependence of surface tension on molecular weight from the effect of end-modification. Films were prepared as described in section 4.3 on cleaned, untreated Si wafers and annealed at 140° C for 6 hours.

Figure 5-10 displays the NR profiles for the 7k dPS/400k PS blend studies. Profiles for the 2, 5, 10 and 20% concentration blends are shown, each offset by a factor of 10 for display purposes. As may be deduced from the high frequency oscillations present in each of the profiles, the thickness of the films used in the blend studies was much larger than thicknesses used for the neat systems. One notable trend present in the NR concentration profiles is the damping

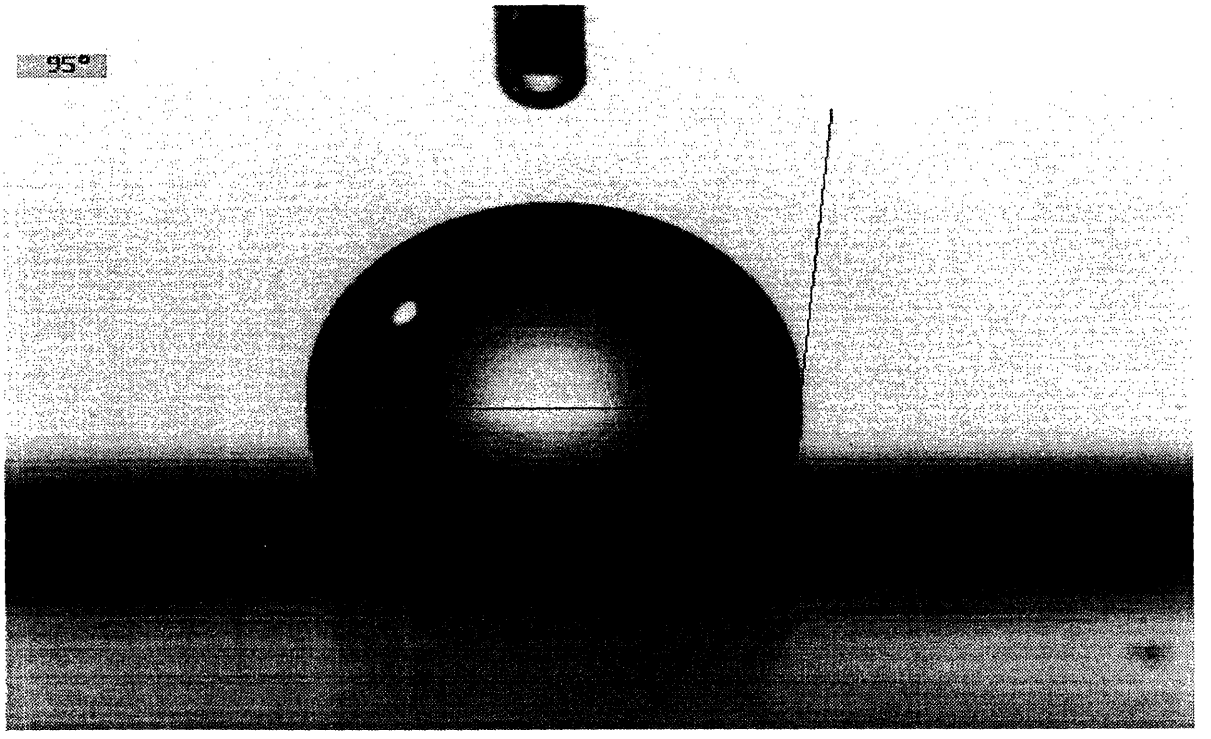

Figure 5-6: 4k PS contact angle measurement. $\theta_e = 95^o$

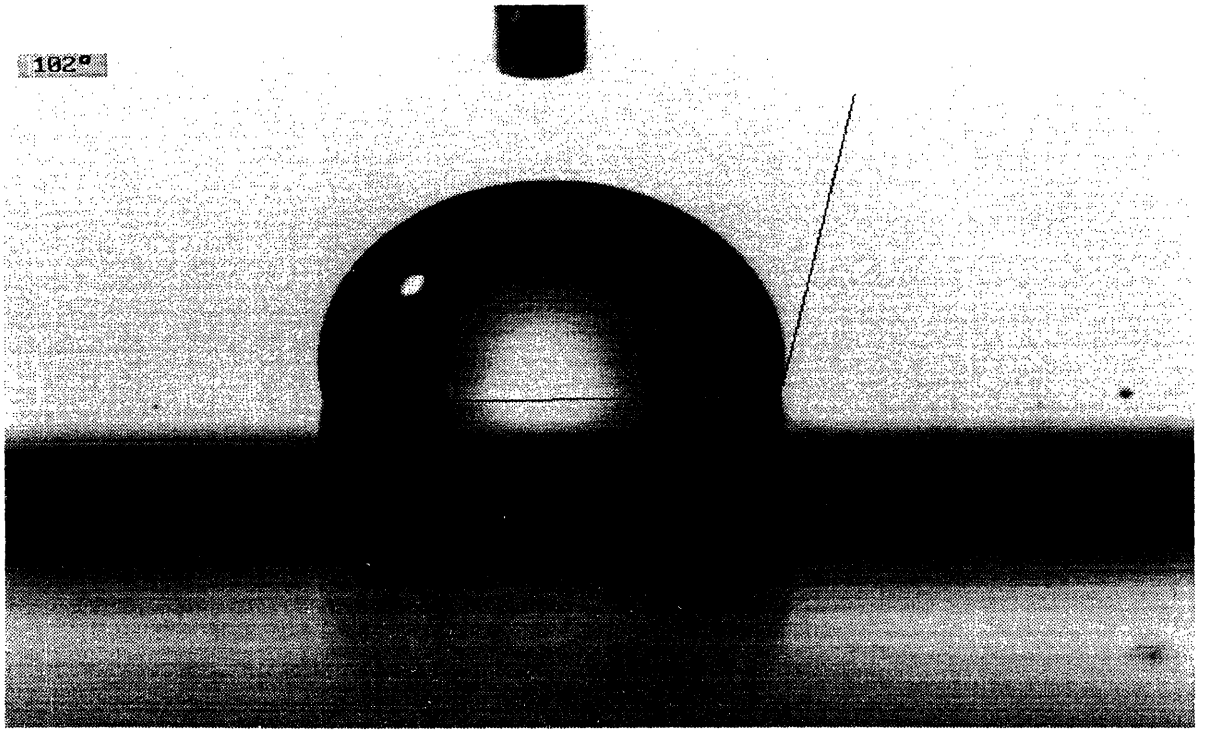

Figure 5-7: 4k PS-TFE contact angle measurement. $\theta_e = 102^o$

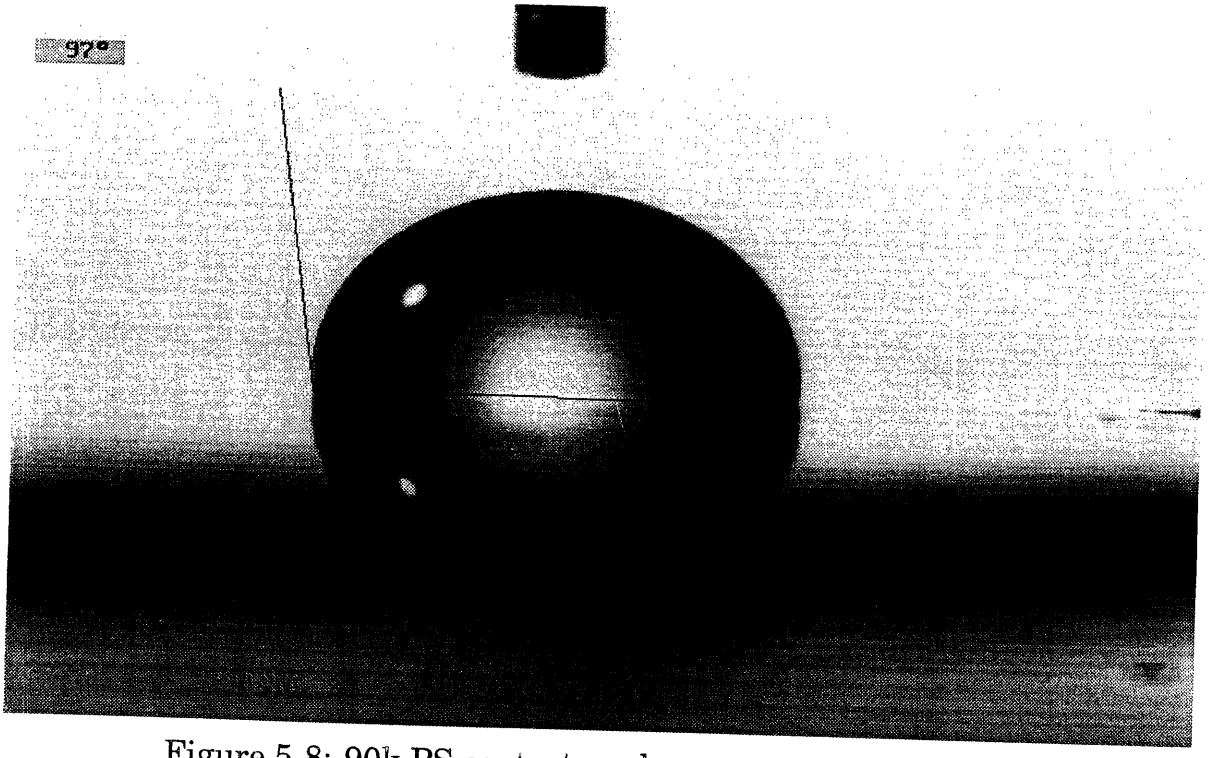

Figure 5-8: 90k PS contact angle measurement. $\theta_e = 97^o$

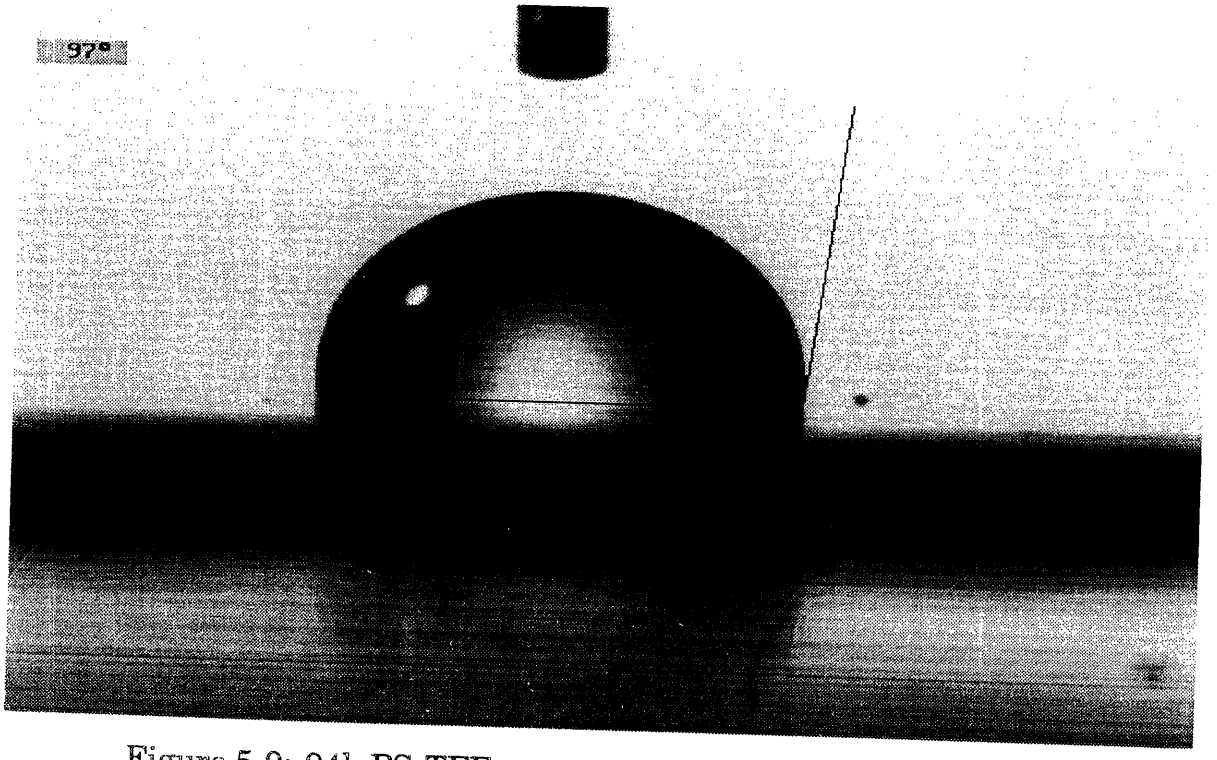

Figure 5-9: 94k PS-TFE contact angle measurement. $\theta_e = 97^o$

of the thickness oscillations as the concentration of the 7k dPS component is increased. This is due primarily to the decrease in contrast between the film and the Si wafer with increasing amounts of dPS. For a 15% dPS/85% PS blend, the b/V is approximately equal to the b/V of Si, hence one would not expect a strongly developed signal from interference fringes in this concentration range.

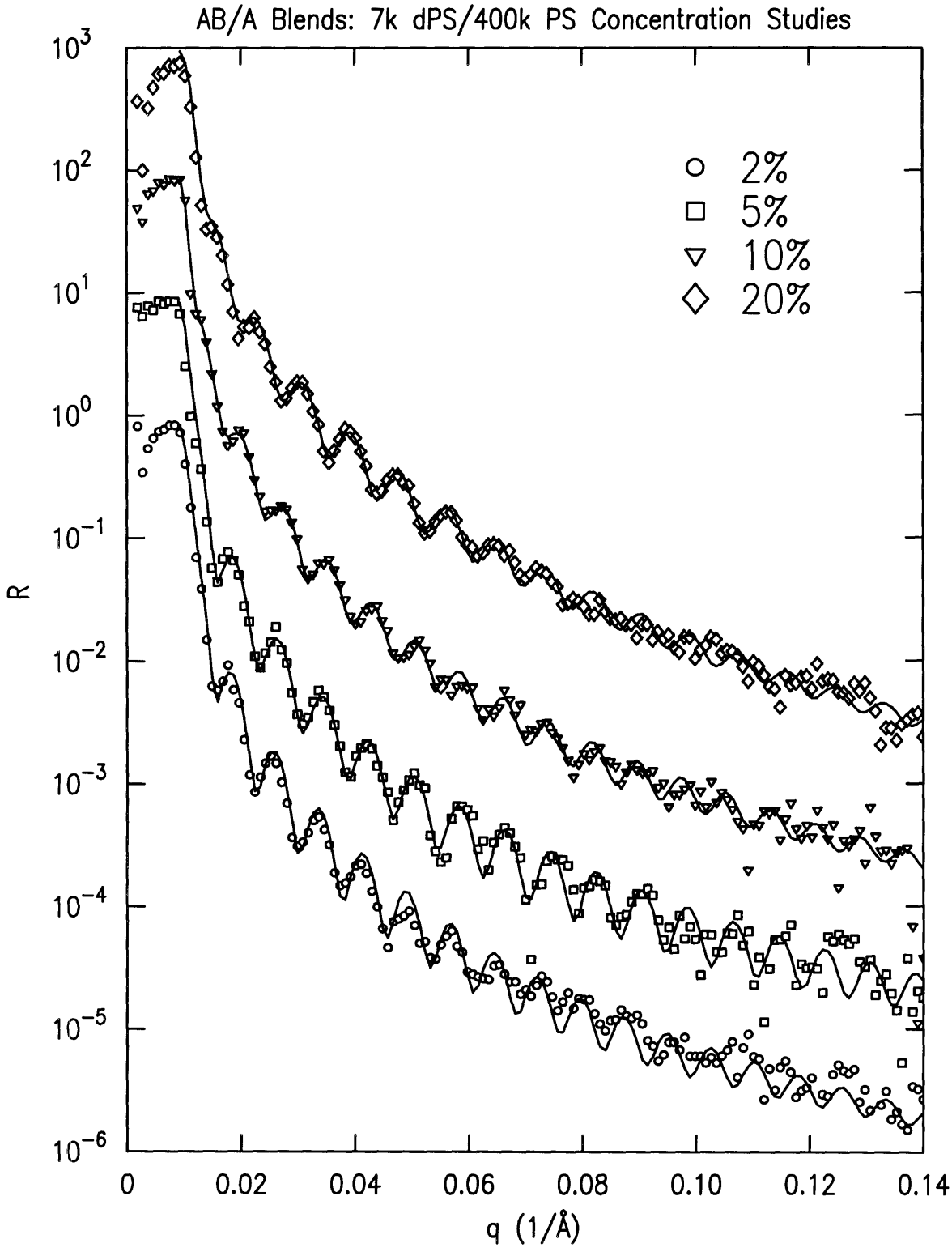

Figure 5-10: NR profiles for AB/A concentration studies

Figure 5-11 displays the NR profiles for the 7k dPS-TFE/400k PS blend concentration studies. Profiles for the 2, 5, 10, and 20% 7k dPS-TFE blends are shown, again offset by factors of 10. In these systems the thickness oscillations are damped even more sharply with increasing concentration of the 7k dPS-TFE material. What is particularly important to note, however, is that compared with profiles from samples with equal concentrations of unmodified 7k dPS, the dPS-TFE systems show greater measured reflectivities at high q. This is clearly indicated by comparing the 20% concentrations for each system at $q = 0.14$. The blend with the end-modified dPS shows a significantly larger measured reflectivity, which is strongly indicative of excess dPS at the film surface.

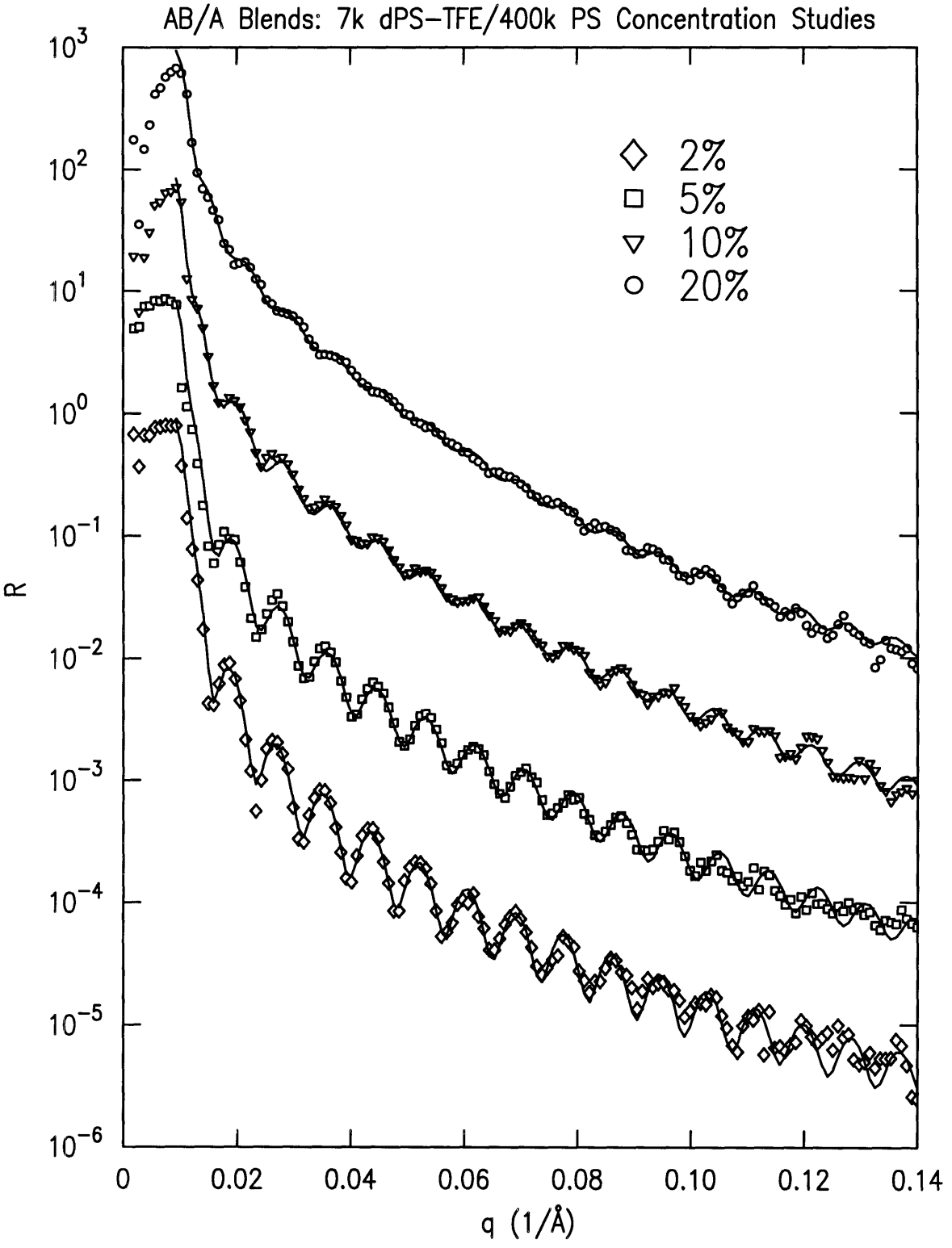

Figure 5-11: NR profiles for AB/A concentration studies

Based on the scattering length density profiles used to generate the fits to the NR data in figures 5-10 and 5-11, the volume fraction profiles of the 7k dPS and 7k dPS-TFE materials in the 400k PS matrix can be determined as a function of sample thickness by using the relation in equation 5.1 where 1 and 2 represent the additive and matrix materials. These volume fraction profiles are shown in figure 5-12 as a function of the normalized sample thickness, L*, which is defined as:

$$L^* = \frac{z}{L} \tag{5.3}$$

where z is the depth perpendicular to the sample surface, and L is the total film thickness. In both cases an enhanced concentration of low molecular weight material can be observed in the region near the substrate, *i.e.* near L*=1.0. The inflection point for the chain distributions averaged $51\mathring{A}$, approximately the coil diameter for the 7k material whose $R_G \approx 24\mathring{A}$. In the control samples, the influence of molecular weight on the surface tension results in a slight excess of the 7k dPS material to the surface (it should be kept in mind that the presence of the butyl-group initiator fragment from the anionic synthesis may also play a role in the segregation). For the blends containing the end-functionalized material, a much larger segregation is observed at the surface due to the low energy chain ends. The fraction of dPS-TFE at the surface increases significantly with bulk concentration, in good agreement with the model predictions of chapter 3.

The degree of excess at the surface can also be shown as a function of thickness, as seen in figure 5-13, where the concentration of low molecular weight material at the surface is normalized by the experimentally determined concentration in the interior of the film. For the 7k dPS blends there is very little enhancement of the low molecular weight additive at the surface for all concentrations. In sharp contrast, the 7k dPS-TFE blends show remarkable surface excesses over bulk levels. The degree of excess is inversely related to the concentration of end-functionalized material in the end-modified blends,

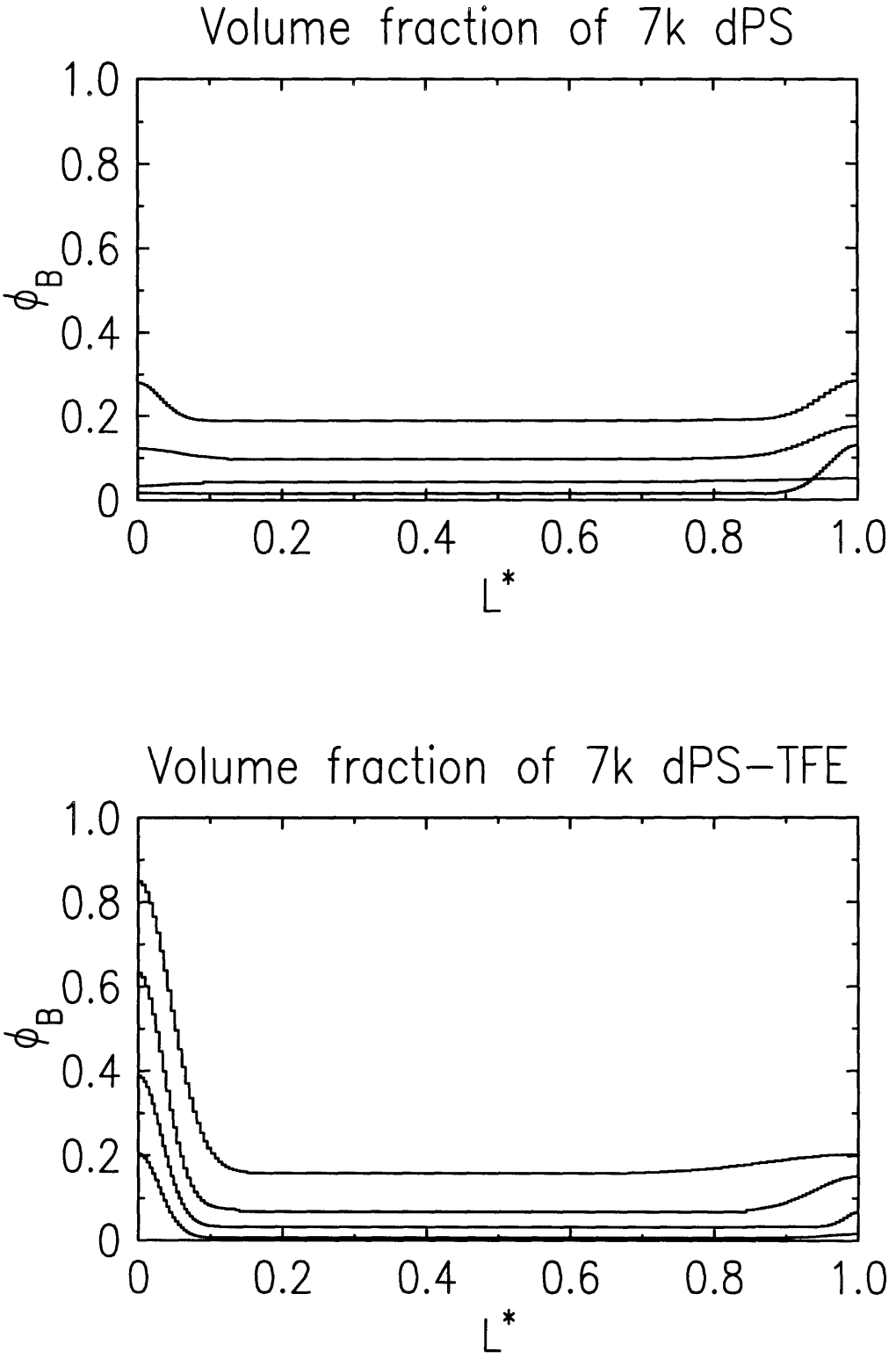

Figure 5-12: Volume fraction of end-functionalized component in AB/A blends.

with the 2% blend demonstrating a surface excess of 30 times and the 20% blend showing a surface excess of just over 5 times the bulk level.

The next set of reflectivity experiments was performed to address the isotopic labelling issue in this investigation. In the previously described experiments the low molecular weight additives were isotopically labelled to provide contrast for the neutrons. The question now addressed centers on whether deuterium labelling provides a favorable surface interaction for that component, since other investigators have noted a selective segregation of dPS in high molecular weight PS/dPS blends [56]. The experiments were carried out with a 6k PS-TFE end-modified polymer and a matrix of 300k dPS. Blend concentrations of 2, 5, and 10% end-functionalized material were prepared as described for the dPS-TFE/PS blends. The resulting reflectivity profiles and corresponding best fits (offset for clarity) are shown in figure 5-14.

The reflectivity profiles are notably different in nature from the previous experiments in two regards. First, the values of the critical angles have nearly doubled to q=0.02 for these profiles, compared to the dPS-TFE/PS blends in figure 5-11. This results from the higher scattering length density of the dPS matrix, as discussed in section 4.2.3. Secondly, the reflectivity at high q values *decreases* with increasing concentration of end-modified material, compared to figure 5-11 which shows the opposite trend. Indeed, comparing the measured reflectivities for the two 10% blends at $q = 0.14\mathring{A}^{-1}$ shows nearly an order of magnitude lower value for the PS-TFE/dPS system, although the average b/V of the film is significantly higher. This data visually suggests that it is the low scattering length density material which localizes at the surface in these blends.

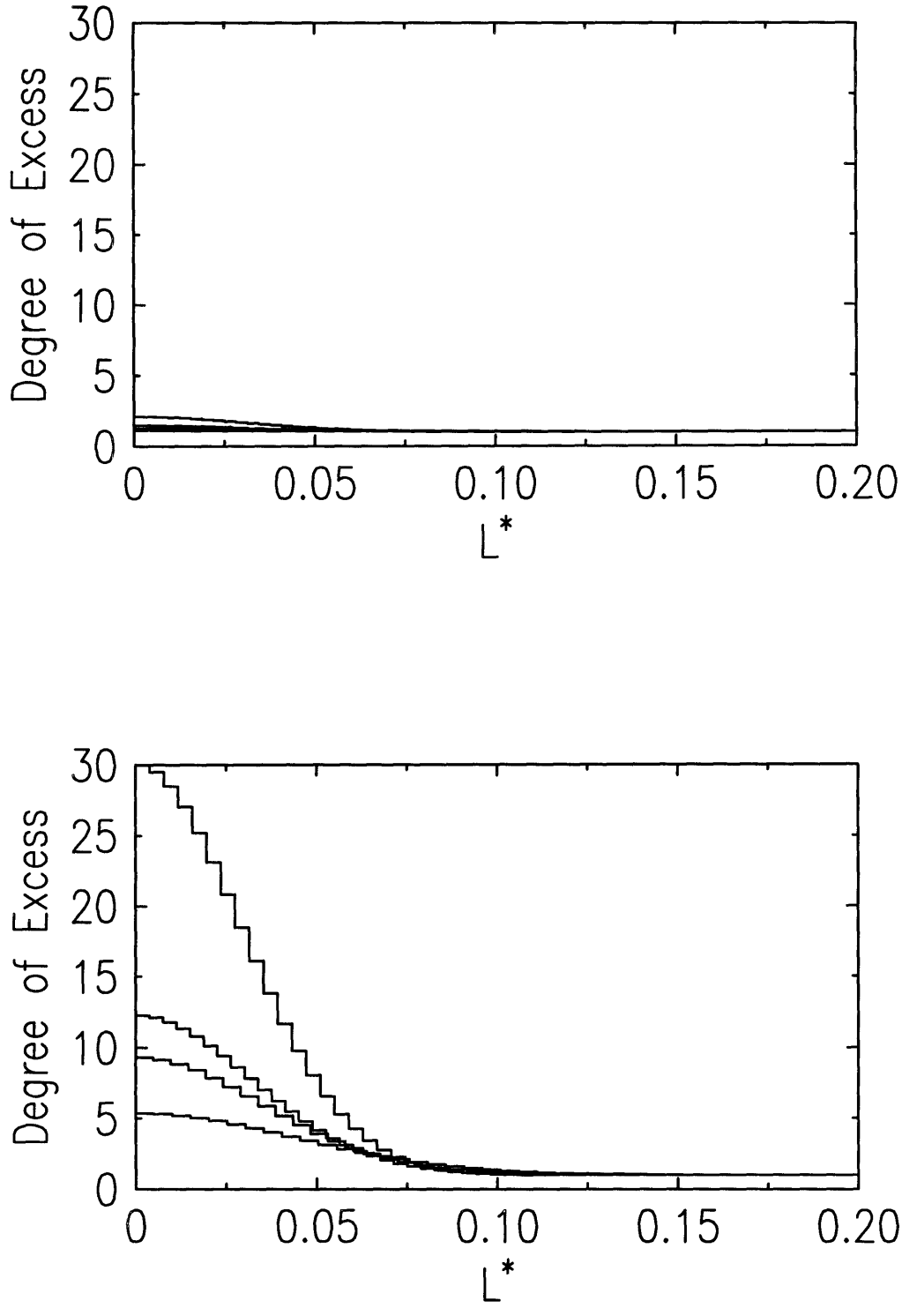

Figure 5-13: Surface excess for the 7k dPS and 7k dPS-TFE blends.

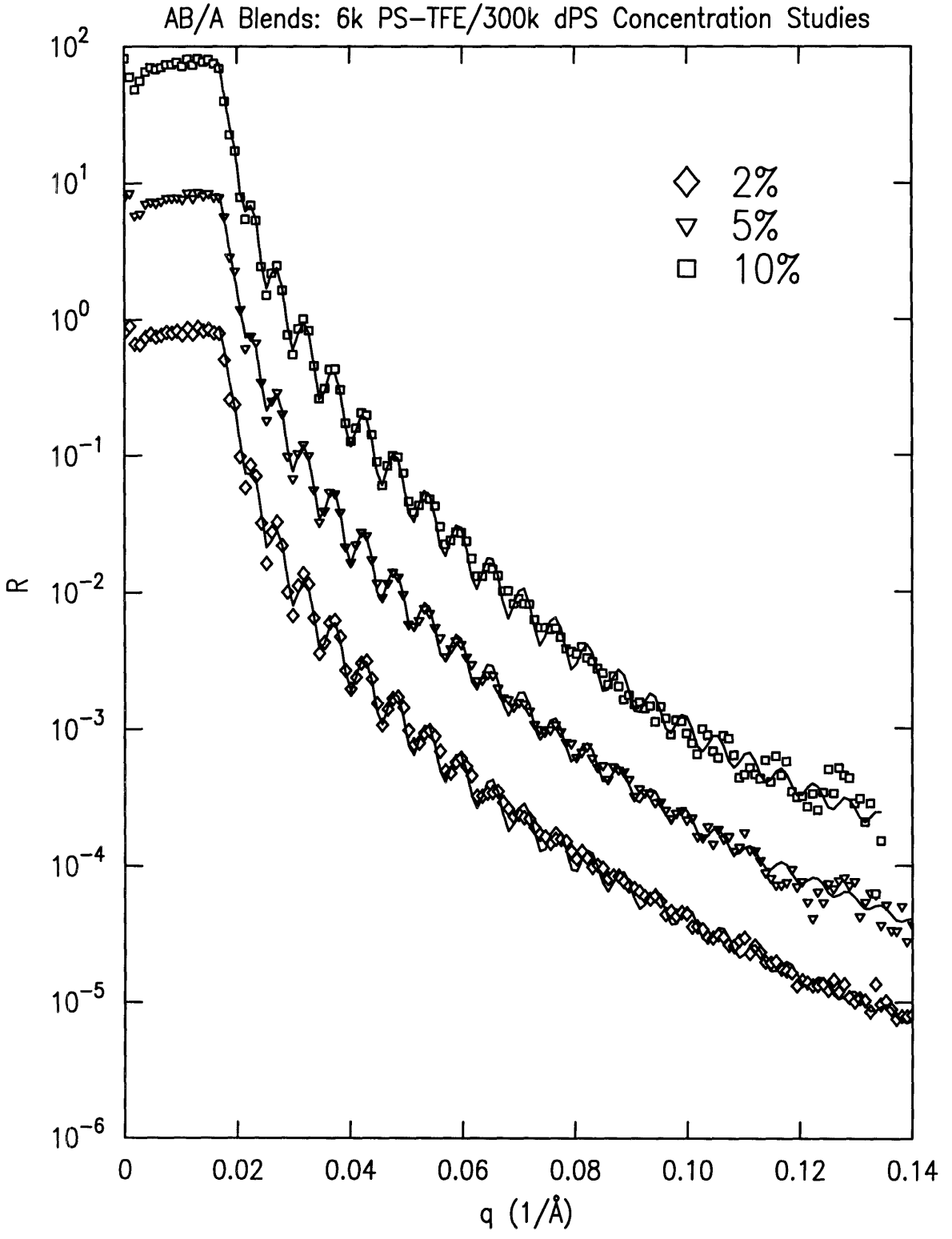

Figure 5-14: NR profiles for AB/A concentration studies

Volume fraction profiles derived from the scattering length density profiles for the 6k PS-TFE/300k dPS blends are presented in figure 5-15. The volume fraction profiles from the earlier 7k dPS-TFE/400k PS blends are repeated for ease of comparison. The nature of the profiles in both cases is identical, with a large enhancement of the low molecular weight end-functionalized additive present at the film surface. Note however, that for a given concentration of end-modified material the surface volume fraction of PS-TFE material is greater than the surface volume fraction of dPS-TFE material. For example, in the 10% samples, the surface concentration of 7k dPS-TFE material is approximately 60% whereas for the 6k PS-TFE material the surface concentration equals 80%. In fact, for any given concentration of additive there is a consistent 20% enhancement of the surface concentration of the PS-TFE additive over the dPS-TFE additive. This variation could be explained by the difference in molecular weight between the two materials. Lower molecular weights would tend to give a higher surface concentration for the same matrix molecular weights, as suggested by the model results in figure 3-2. Since the matrix molecular weight is also lower however, this effect would tend to be cancelled out. The difference in surface coverage could alternatively be explained by the difference in sample thicknesses, which for the PS-TFE blends averaged 1072$\mathring{A}$ compared to 736$\mathring{A}$ for the dPS-TFE blends. According to the model results in chapter 3, figure 3-4, greater thicknesses give a higher degree of surface coverage under identical concentration and molecular weight conditions. Regardless, no selective segregation of dPS to the surface was observed. The results seem to suggest isotopic effects are negligible in our systems.

The surface excess plots for the blends are presented in figure 5-16, along with analogous plots from the 7k dPS-TFE/400k PS system for comparison. Results for the 2, 5, and 10% blends are displayed for both series of blends. In the case of the 2% blends, there is a large disparity between the dPS-TFE and PS-TFE blends, with the dPS-TFE blend portraying roughly twice the degree of excess as the PS-TFE blend. The surface excesses for the 5 and 10% samples

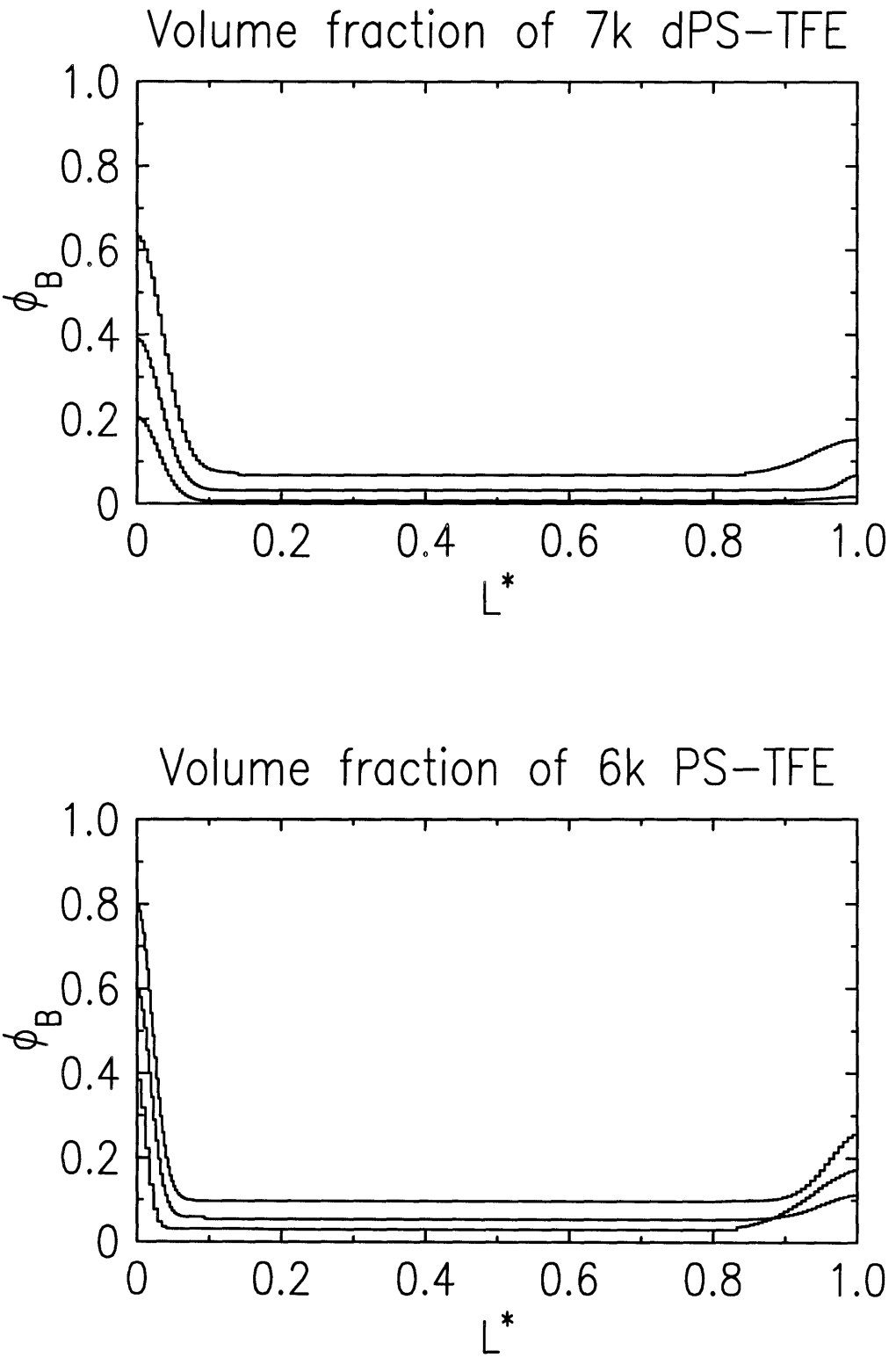

Figure 5-15: Volume fraction of end-functionalized component in AB/A blends.

Table 5.1: Summary of 7k dPS-TFE/400k PS Concentration Studies

system	experimental φ_β	surface concentration	surface excess	near-surface region depth
2%	2.1%	20.42%	30	87$\mathring{A}$
5%	5.19%	38.89%	12.25	82$\mathring{A}$
10%	10.09%	63.25%	9.3	106$\mathring{A}$
20%	20.36%	84.9%	5.35	114$\mathring{A}$

show essentially equal degrees of enhancement. The other noteworthy remark to make in regards to these results is the size of the enhancement regions; the PS-TFE blend enhancement regions appear to be consistently shorter by approximately 30% than the dPS-TFE blends for the entire concentration range. This is primarily due to the normalization procedure and to the difference in sample thicknesses.

To summarize the NR results of the AB/A blend studies, figure 5-17 displays the surface concentration of the low molecular weight component versus the bulk concentration for the PS-TFE, dPS-TFE and control dPS blends. In a design application one may wish to maximize the extent of surface coverage of the low energy TFE tails, using the minimal amount of end-modified material. Figure 5-17 shows that for a given bulk concentration of end-modified PS, the 6k PS-TFE additive is more efficacious than the 7.4k system, suggesting that for smaller molecular weights, even larger surface coverages are achievable. The second interesting observation from figure 5-17 is the magnitude of the difference in surface coverage between end-modified materials and a low molecular weight PS analog. Clearly, molecular weight effects appear to be negligible relative to the effect of the low energy tail. This suggests that (1) minimal segregation will be observed at the surface of a polydisperse homopolymer system and, (2) using conformational effects alone to produce a surface coverage of functional ends *in linear chain systems* would not appear feasible. These results are summarized in tabular form in tables 5.1 and 5.2.

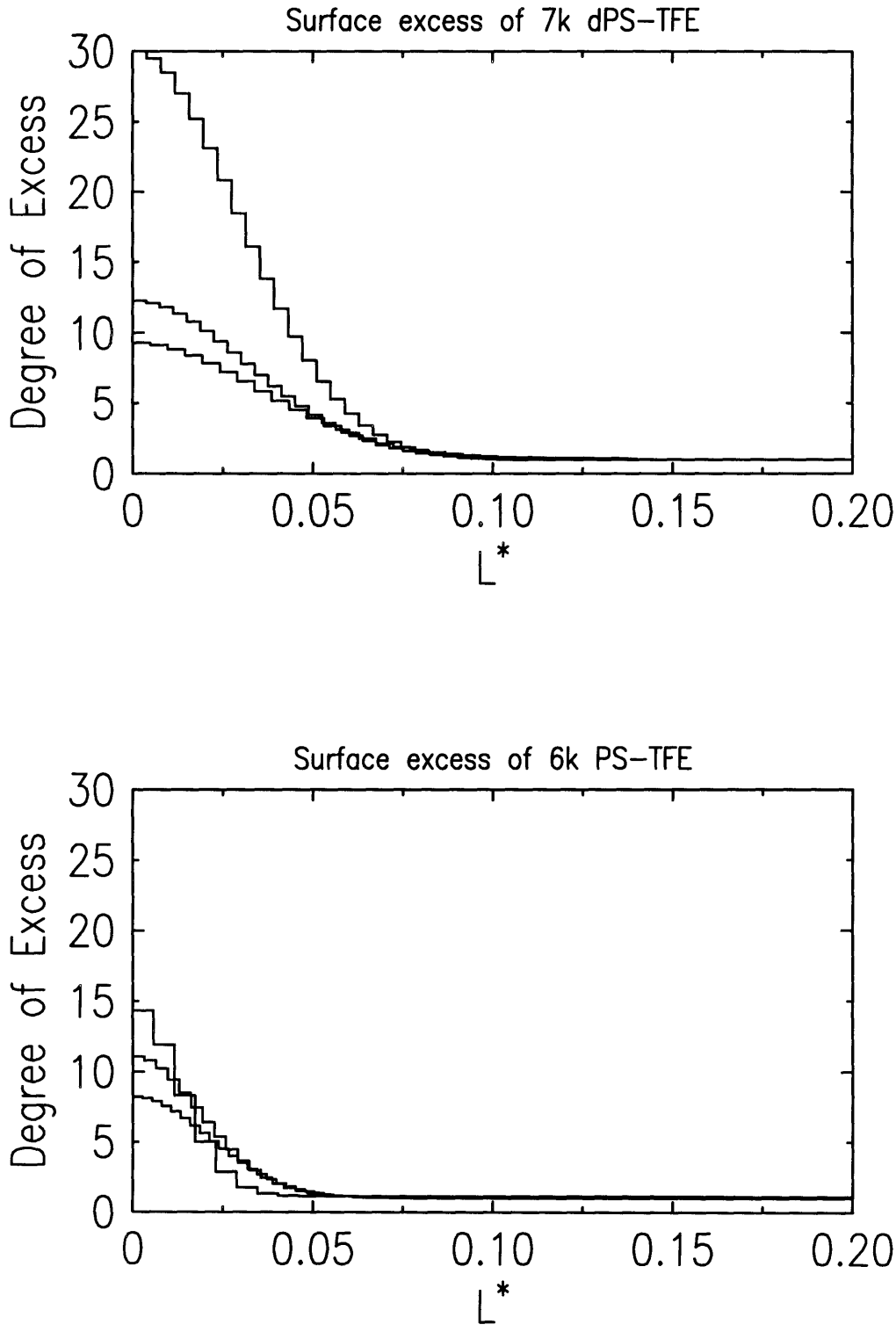

Figure 5-16: Surface excess for 7k dPS-TFE and 6k PS-TFE blends.

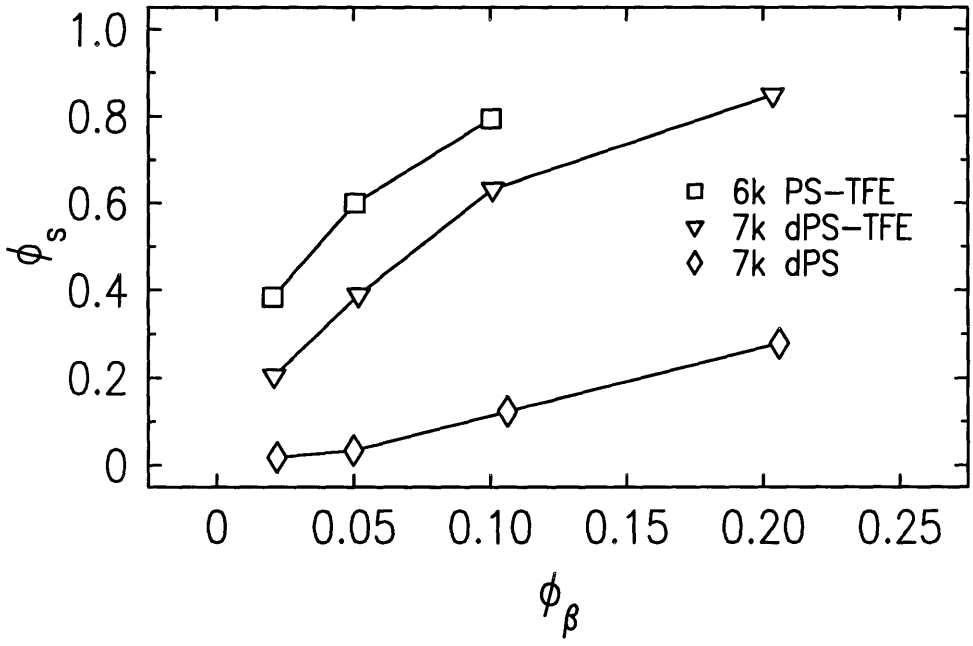

Figure 5-17: Summary of AB/A blend studies.

Table 5.2: Summary of 6k PS-TFE/300k dPS Concentration Studies

system	experimental φ_β	surface concentration	surface excess	near-surface region depth
2%	2.05%	38.37%	14.3	65.8Å
5%	5.05%	60%	11.1	102Å
10%	10.04%	79.4%	8.2	84Å

5.2.2 Contact Angle Measurements

Contact angle measurements were conducted on the blend systems used in the NR experiments. These measurements were taken in the same manner as in the contact angle measurements described in section 5.1.3. The results for the 7k dPS/400k PS and 7k dPS-TFE/400k PS blends are shown in figure 5-18. The dPS/PS blends show essentially no dependence of contact angle on the bulk concentration of 7k dPS material. In the case of the dPS-TFE/PS blends, the contact angle is an increasing function of the bulk concentration of end-functionalized material. These results are qualitatively in agreement with the volume fraction profiles derived from the NR experiments, displayed in figure 5-12, where it was shown that for the range of concentrations used, the surface volume fraction of the 7k dPS material was essentially constant, while the surface volume fraction of 7k dPS-TFE material increased with increasing bulk concentration. However, the actual measured values are low relative to what one would expect from the contact angle measurements on the pure systems, presented in figure 5-5.

One reason to account for this discrepancy may be the molecular weight dependence of the surface tension, which should give somewhat lower θ_e values for the dPS/PS blend systems. However, this does not adequately explain the results for the dPS-TFE/PS blends, where even for the 20% sample, where the dPS-TFE surface concentration reached 85%, the contact angle is approximately 5 degrees less than the neat, thin film system. Room temperature variations may account for these results, as measurements on the dPS/PS and dPS-TFE/PS were carried out on a different date from the other contact angle measurements in this study. Increases in the room temperature will cause decreases in the observed contact angle. The advancing contact angle for H_2O on PS at 20°C is cited as 91° in reference [9], well below the values observed in this study.

The results for the contact angle measurements on the 6k PS-TFE/dPS

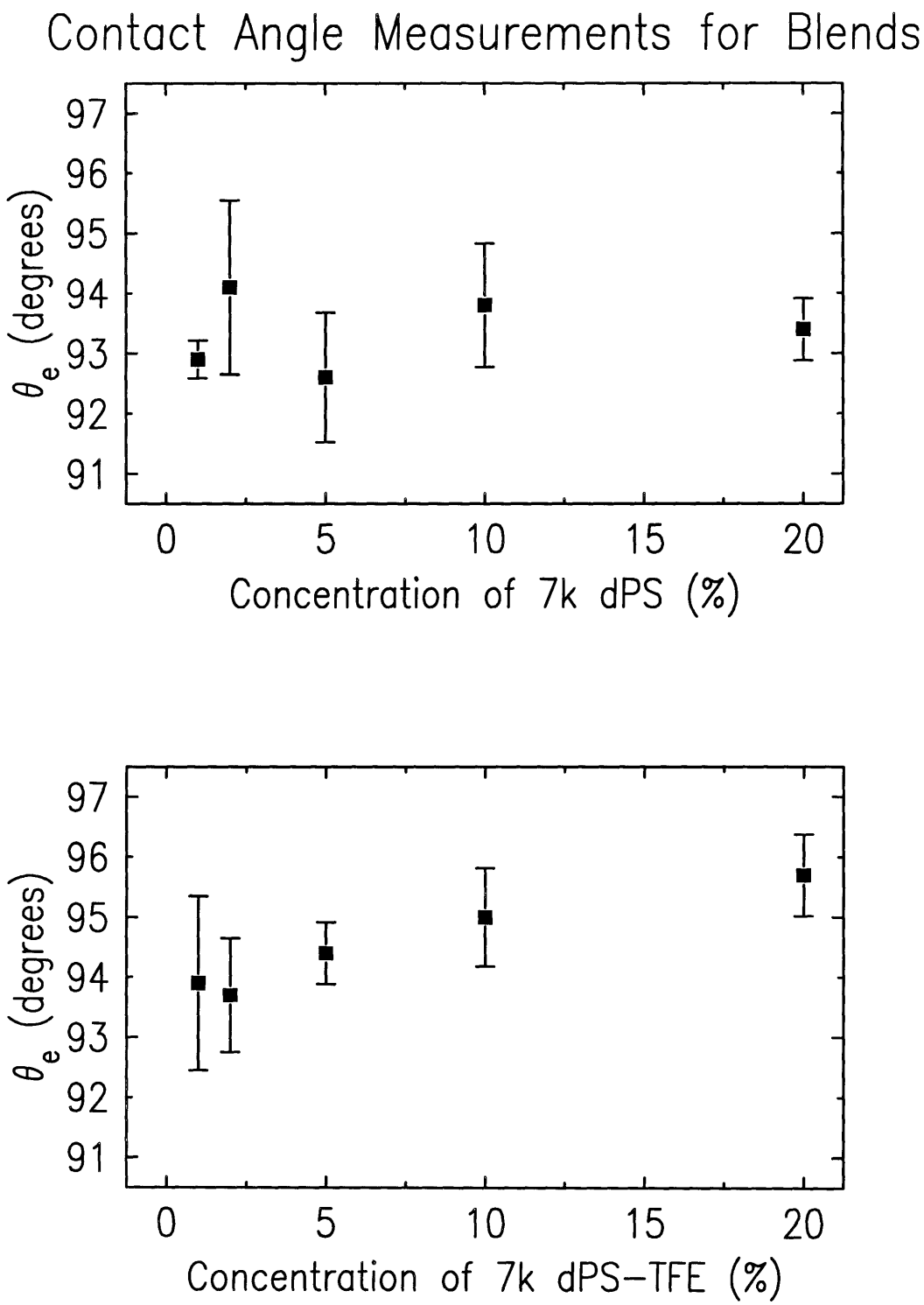

Figure 5-18: Contact angle measurements for PS matrix blends.

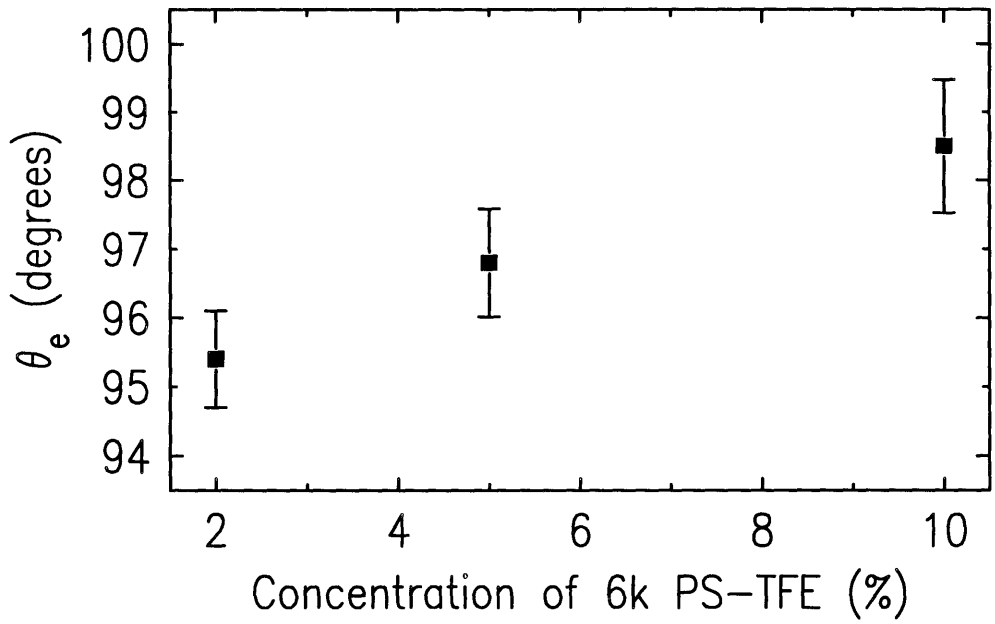

Figure 5-19: Contact angle measurements for dPS matrix blends

blends are shown in figure 5-19. A monotonically increasing contact angle with increasing bulk concentration of end-modified PS-TFE is seen, similar to the dPS-TFE blends in figure 5-18. This result corroborates the NR results shown in figure 5-15 where it was seen that for increasing bulk concentration of 6k PS-TFE material, the surface volume fraction increased significantly. A comparison between the contact angle measurements for the PS-TFE blends and the dPS-TFE blends from figure 5-18 reveals that the magnitude of the contact angles are significantly larger for the PS-TFE blends, and in reasonable agreement with the data presented in figure 5-5. For instance, the 10% blend of 6k end-modified material gives a measured contact angle of 98.5°, suggesting a TFE-tail coverage of 17% based on equation 5.2. In comparison, the pure system gave an angle of 100.5°, corresponding to a TFE surface concentration of 26%. (This value also agrees with the calculated value of 26% from equation 2.5, assuming two equivalent segments of TFE at the surface for each end-modified chain.) The NR data indicates 80% PS-TFE resides at the blend surface. Hence the expected surface concentration of TFE is (26%)·(80%) or 21%, in good agreement with the contact angle measurements for the blend.

Chapter 6

Conclusions

Based on the results presented in chapter 5 several conclusions can be drawn on the studies we have conducted:

- Thin films of PS-TFE polymers on the order of $4R_G$ or less in thickness exhibit complete segregation of chain ends to the air surface and substrate interface.
- PS-TFE systems below $M_n = 30,000$ exhibit measurably lower surface energies compared with unmodified polystyrene.
- Surface segregation in blends of PS-TFE with PS is dominated by the energetic savings from the localization of low energy chain ends at the air surface. The molecular weight dependence of surface tension appears to play a negligible role in the segregation phenomena observed herein, as does the isotopic labelling.
- Film thickness has a significant influence on the degree of segregation, with thicker films exhibiting more segregation.

Chapter 7

Recommendations for Future Work

Based partly on the results of this investigation, chain end segregation appears to hold promise as a new method of surface modification. This is particularly so when end-functionalized polymers, such as those used in this thesis, are to be employed. In our study, we focused on end-segregation of low energy tails, this type of segregation may be of interest for applications requiring anti-stain, low friction, anti-fouling or low adhesion surfaces. Using other end groups, different functionalities can be achieved. Recently [33] for example, Norton et al. utilized a series of carboxylic acid terminated polystyrene (PS-COOH) samples to enhance adhesion at a thermoset-thermoplastic interface. Since the end-functionalized tail grafts to the epoxy resin, a large increase in fracture toughness may be expected to result. Their studies showed that for the optimized surface density of PS-COOH, an increase of over 20 times the bare interfacial fracture toughness was achieved. This promising result is just one example of other potential directions for continuing work on chain end segregation.

Since one objective is maximizing surface coverage of functional ends, it may be interesting to explore in future investigations the behavior of materials functionalized at both chain ends rather than one end as in our experiment.

This modification could be carried out for end-functionalized styrene polymers by using naphthyllithium as a di-initiator in the anionic polymerization rather than *sec*-butyllithium. The result would make an interesting complement to these investigations as it would isolate the role the initiator fragment plays in our experiments.

A continuation of the AB/A blend studies begun in this work would provide more information on the competition between the entropy of mixing of the two components, and the reduction in surface energy driving the end-functionalized polymers to segregate. This could be carried out by varying the molecular weight of the polystyrene matrix as well as that of the end-functionalized PS. Entropy should play a larger role in mixing as the molecular weight of the matrix is reduced because the entropic contribution is inversely dependent on the size of each blend constituent. Lowering the matrix molecular weight to a size comparable with the end-functionalized polymers would increase their tendency to mix. Based on the difference in coverage observed between the 7.4k dPS-TFE and 6.3k PS-TFE blends, lower molecular weight end-functionalized additives may provide even higher surface coverage at low bulk concentrations, useful from the standpoint of industrial applications.

Finally, it would be interesting to study the effects of chain end segregation in thin films on T_g. As observed in these investigations, the low molecular weight

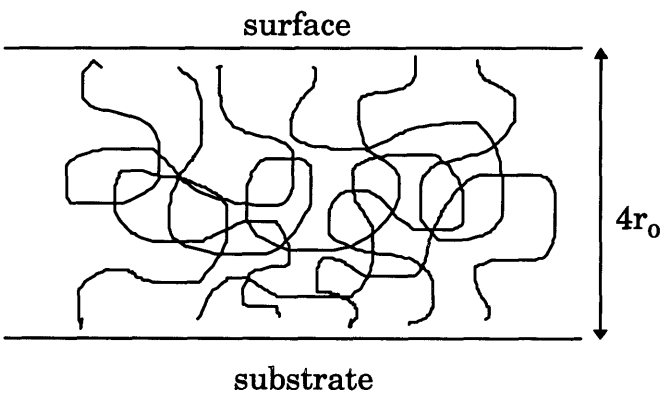

Figure 7-1: Thin film sample exhibiting complete chain end segregation.

end-functionalized polymers exhibit complete segregation of chain ends to the air surface and substrate interface when the film thickness is approximately $4R_G$. As a result, the interior of the film is entirely absent of chain ends, as seen schematically in figure 7-1. Recalling the T_g dependence on molecular weight (see equation 2.6) due to the contribution from chain ends, the lack of chain ends in the film interior should result in a higher T_g that approaches $T_{g,\infty}$. Such a prediction could be measured using x-ray reflectivity.

Appendix A

Free Energy Model Source Code

```
C
C  PROGRAM TO CALCULATE THE FREE ENERGY OF THE NEAR-SURFACE SEGREGATION
C  REGION.  FREE ENERGY IS MINIMIZED IN ETA (FRACTION OF 'A' MONOMER
C  FROM END-MODIFIED POLYMER IN THE NEAR SURFACE REGION), AND GAMMA
C  (FRACTION OF END-MODIFIED POLYMER SEGREGATING TO NEAR SURFACE
C  REGION).
C

      PROGRAM INTERFACE

                                                                      10
      INTEGER I,J,K
      DOUBLE PRECISION ETA,GAMMA,LAMB,PHI,
     $  PHI1,INT,MIX,DEF,NA,NB,H,DTFE,PI,FOUT,
     $  ETAO,NFTOT,FMIC,FTOT,NT,NH,FA,FB

      DOUBLE PRECISION DLOG,DSQRT
      INTRINSIC DLOG,DSQRT

      PI = 3.14159265

                                                                      20
C *****INITIALIZE VARIABLES*****
      A = 6.7
      H = 750.0
```

```
      FA = 0.9692
      FB = 1.-FA
      NT = 3856.
      NA = FA*NT
      NB = FB*NT
      NH = 3856.
                                                                      30
C *****LOOK THROUGH POSSIBLE PHYSICAL VALUES FOR MINIMUM*****
      DO 30 K = 1,20
        PHI = 0.01*K
    FTOT = 1.0
      DO 10 I = 1,99
            ETA = I*0.01
            DO 20 J = 1,99
              GAMMA = J*0.01
              LAMB = FA/ETA + FB
          PHI1 = PHI*(1.-GAMMA)/(1.-PHI*GAMMA*LAMB)                   40
              DTFE = 2.*H*PHI*GAMMA/(NT*A)

C *****COMPUTE VALUES FOR EACH OF THE FREE ENERGY TERMS*****
      INT = (3.3245-(1.869*ETA)/(NT**0.667)-((1.-ETA)*1.869)/
     1          (NH**0.667))*(A/H)+(2.*PHI*GAMMA*(1/NT)*(0.803-3.3245+
     2          (ETA*1.869)/(NT**0.667)+((1.-ETA)*1.869)/
     3          (NH**0.667)))

      DEF = GAMMA*(1/NT)*PHI*((1.5*(GAMMA*LAMB*H*PHI)**2)/(NA*(A**2))
     1          +((PI**2)*NA*A**2)/(6*(GAMMA*LAMB*H*PHI)**2))          50

      MIX = PHI*GAMMA*LAMB*(ETA*DLOG(ETA)/NA +
     1  (1.-ETA)*DLOG(1.-ETA)/NH)

      FOUT = (1.-PHI*GAMMA*LAMB)*(PHI1*DLOG(PHI1)/NT
     1  + (1.-PHI1)*DLOG(1.-PHI1)/NH)

      FMIC = INT + DEF + MIX
```

```
      NFTOT = FMIC + FOUT                                              60

C *****CHECK TO SEE IF THE FREE ENERGY IS LOWEST*****
      IF (NFTOT.LT.FTOT) THEN
      FTOT = NFTOT
      ETAO = ETA
      GAMMAO = GAMMA
      ENDIF
 20           CONTINUE
 10   CONTINUE
                                                                       70
C *****WRITE THE OUTPUT TO A FILE*****
        WRITE(*,*)PHI,ETAO,GAMMAO,DTFE,FTOT
 30   CONTINUE

      STOP
      END
```

Appendix B

GPC Chromatograms of End-Modified Polystyrenes

GPC chromatograms are shown here for the polymers synthesized in 4.1.1.

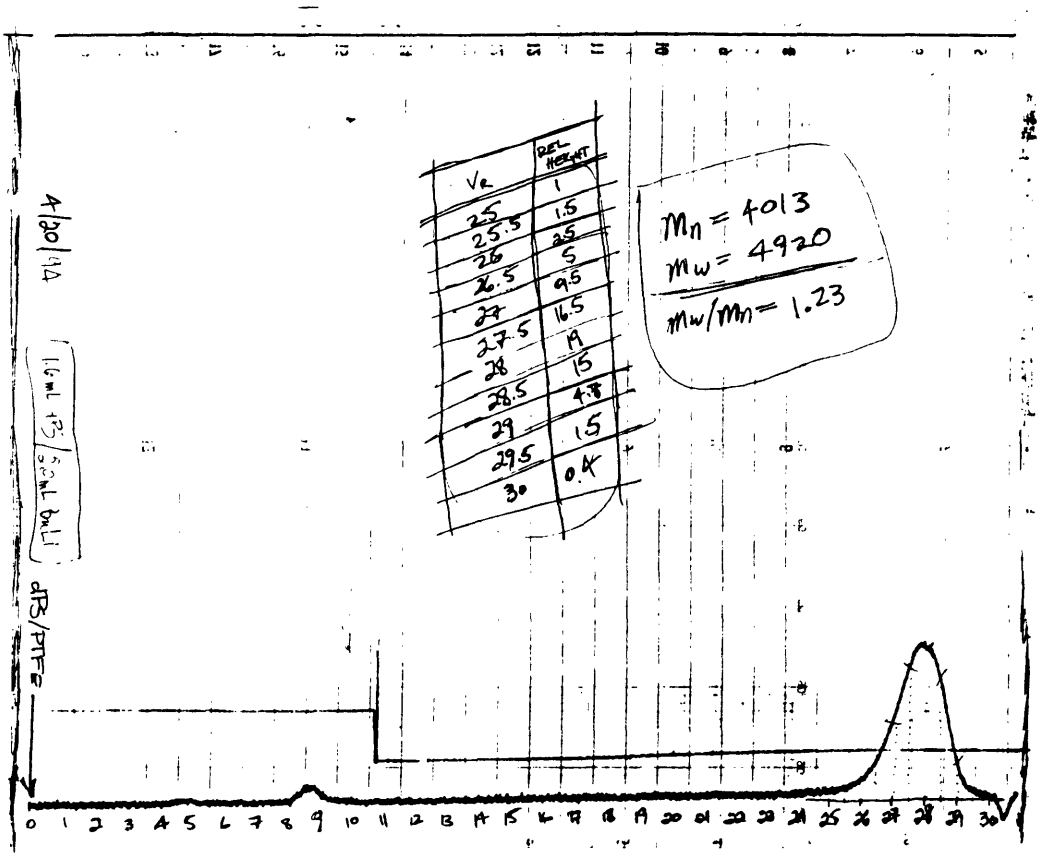

Figure B-1: GPC chromatogram of sample #1.

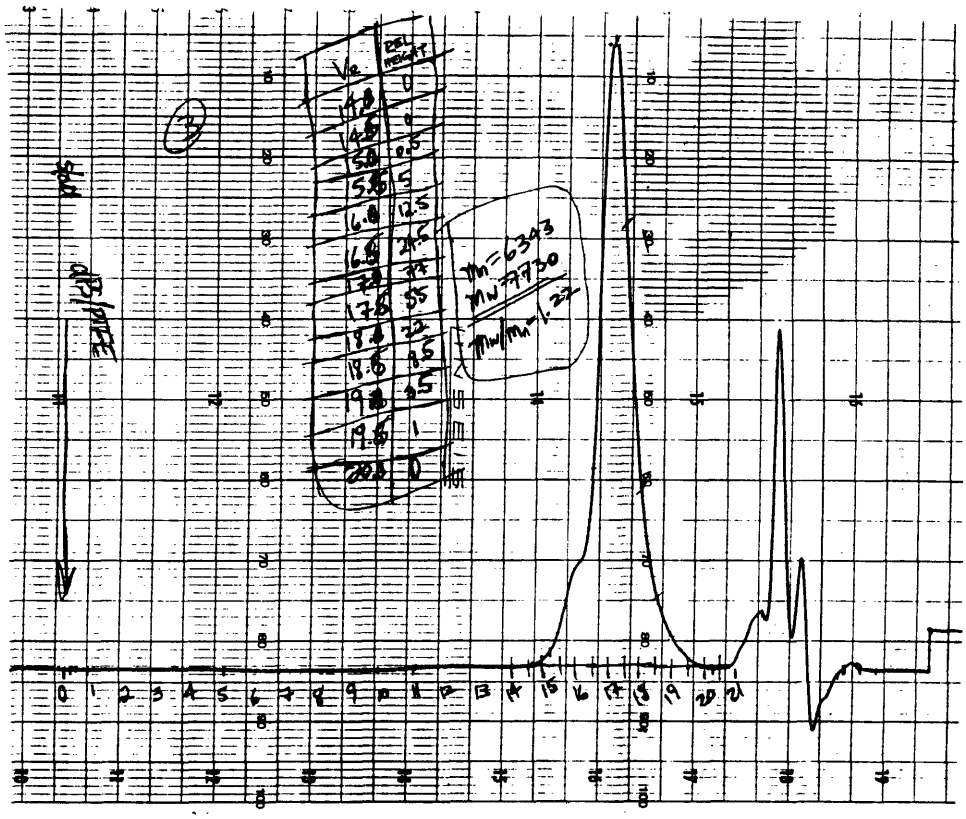

Figure B-2: GPC chromatogram of sample #2.

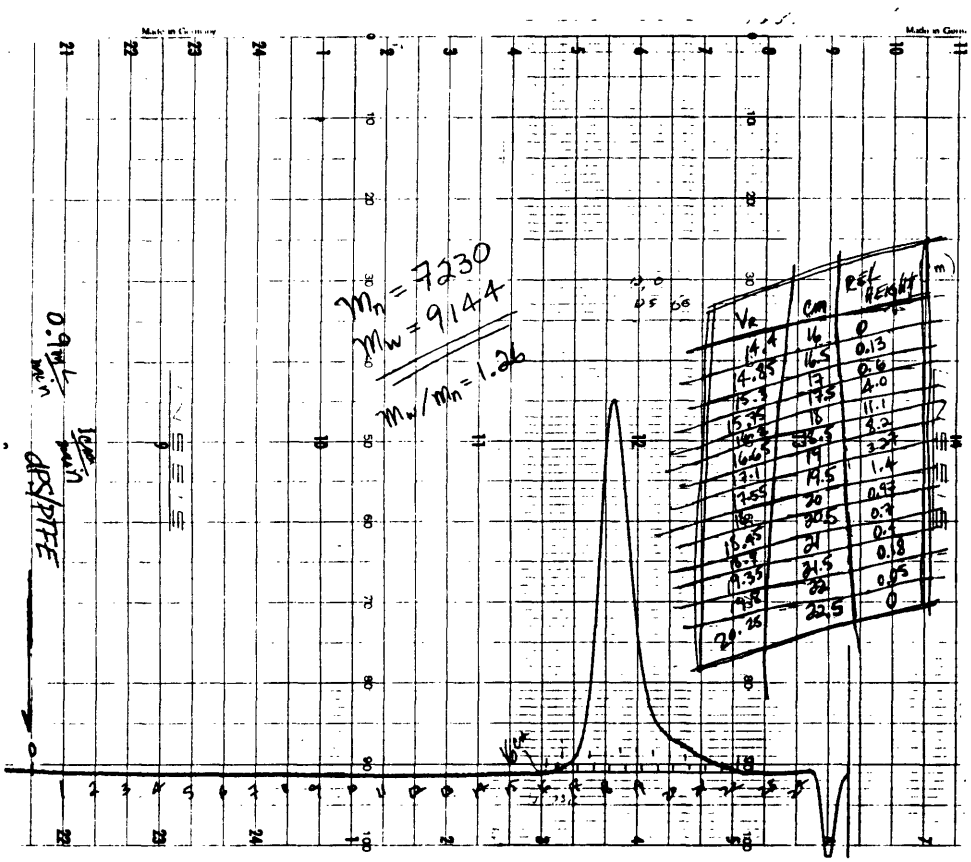

Figure B-3: GPC chromatogram of sample #3.

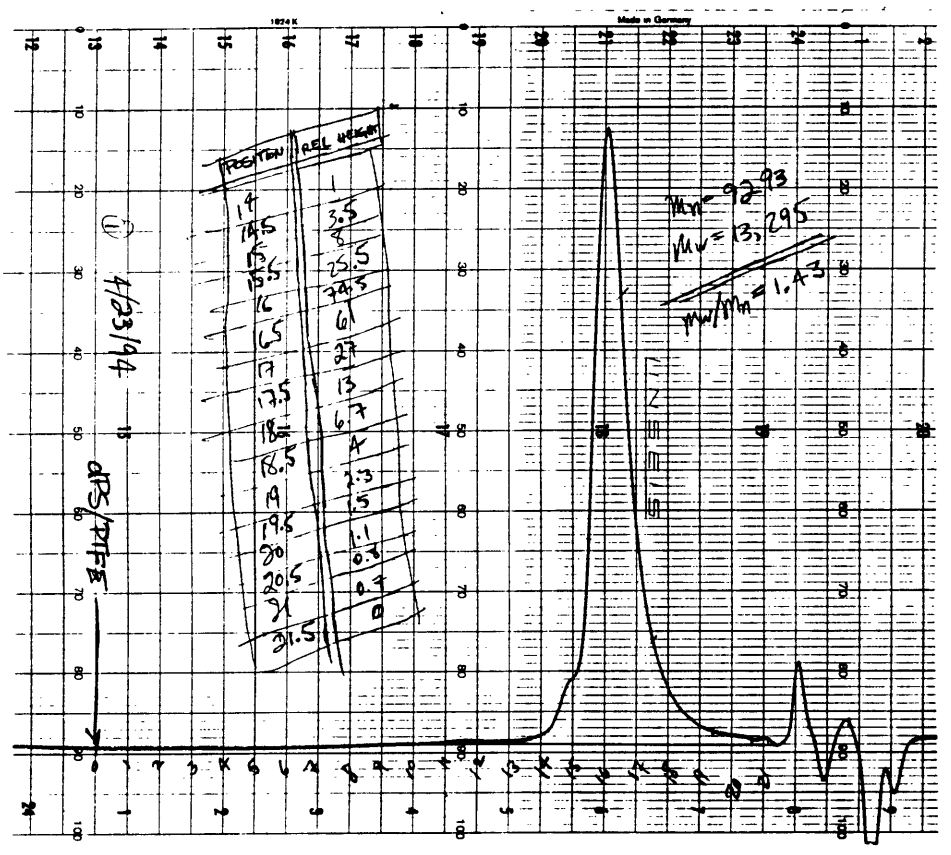

Figure B-4: GPC chromatogram of sample #4.

Appendix C

NMR Spectra of Selected End-Modified Polystyrenes

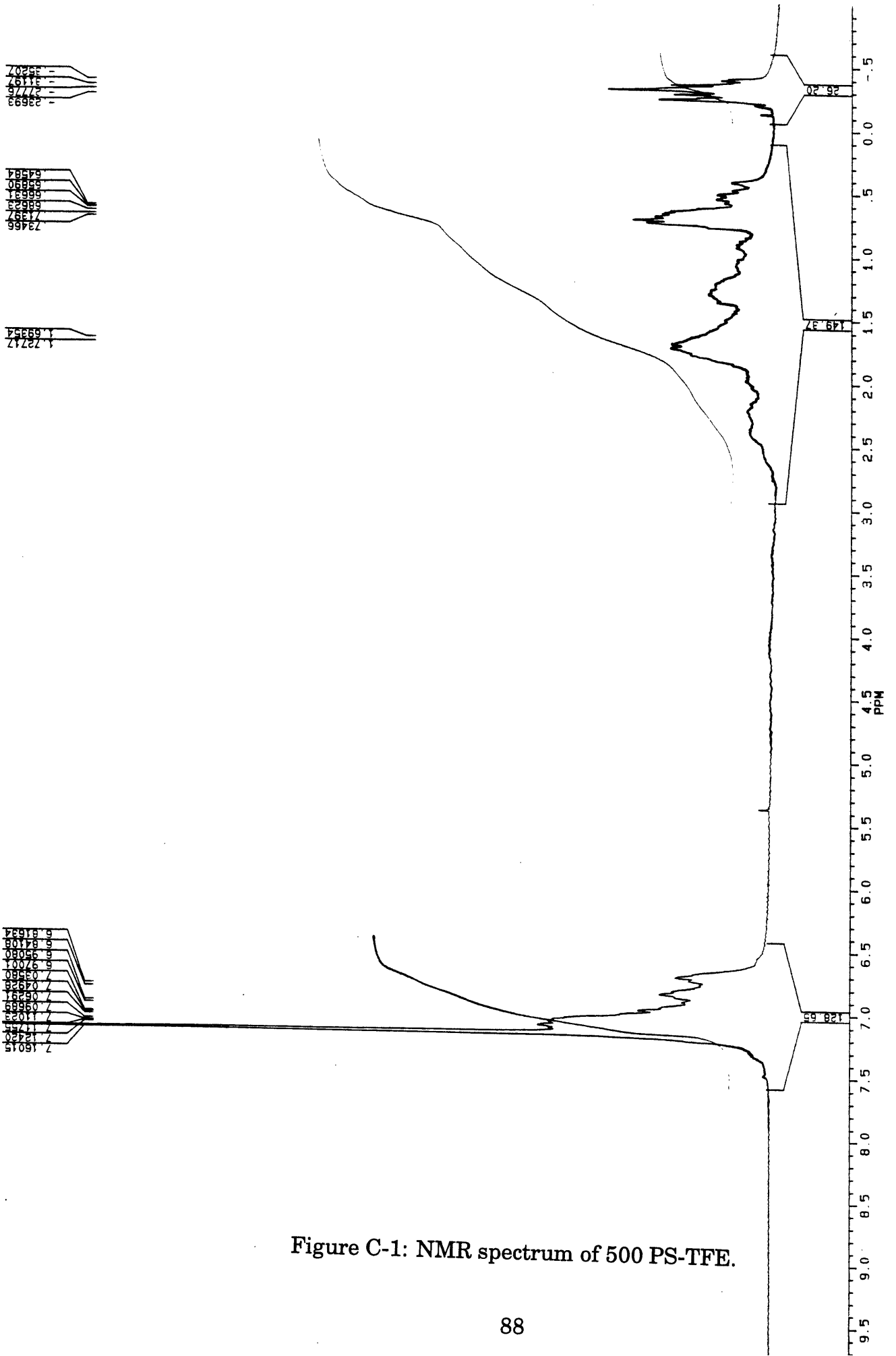

Figure C-1: NMR spectrum of 500 PS-TFE.

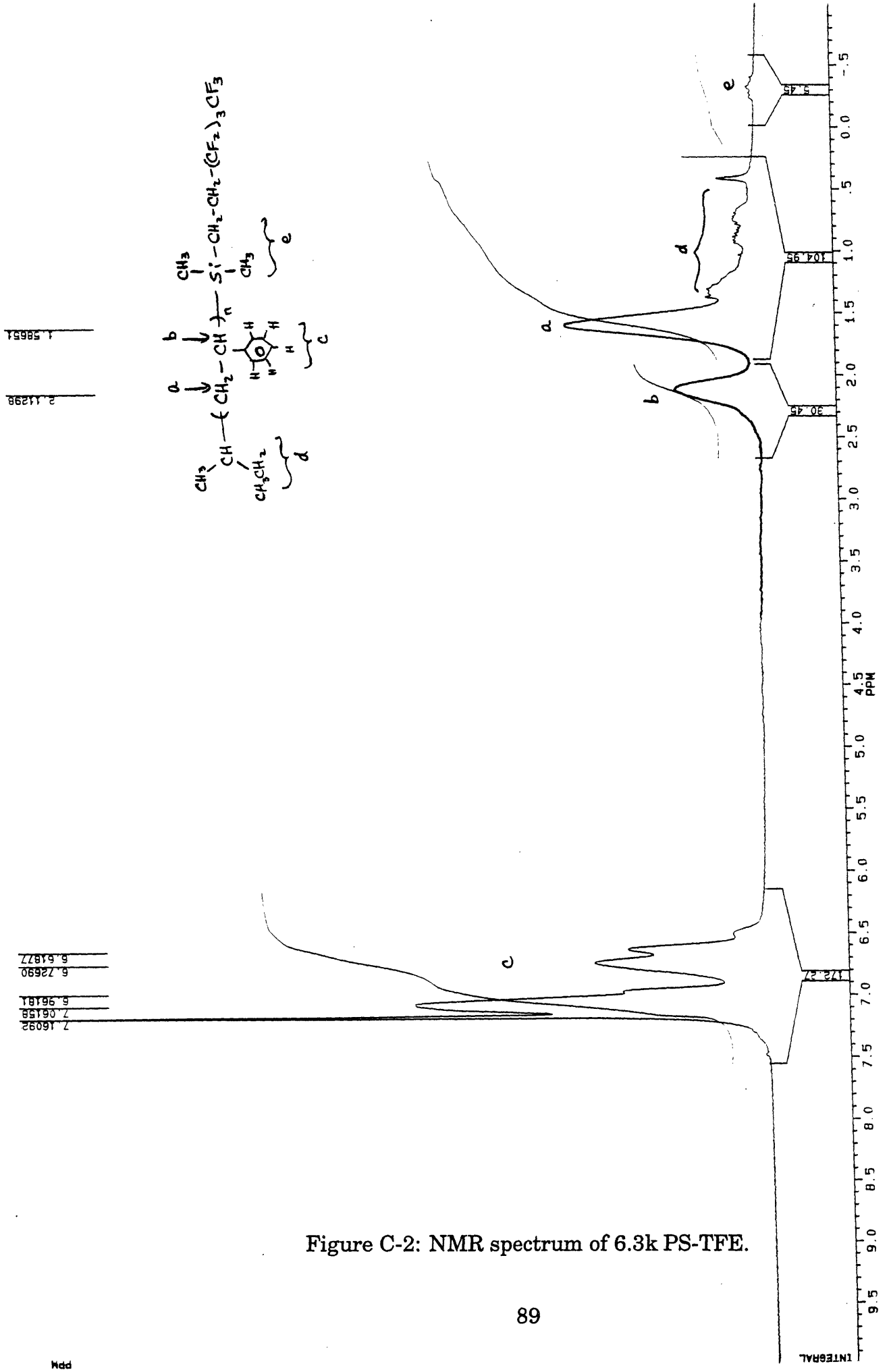

Figure C-2: NMR spectrum of 6.3k PS-TFE.

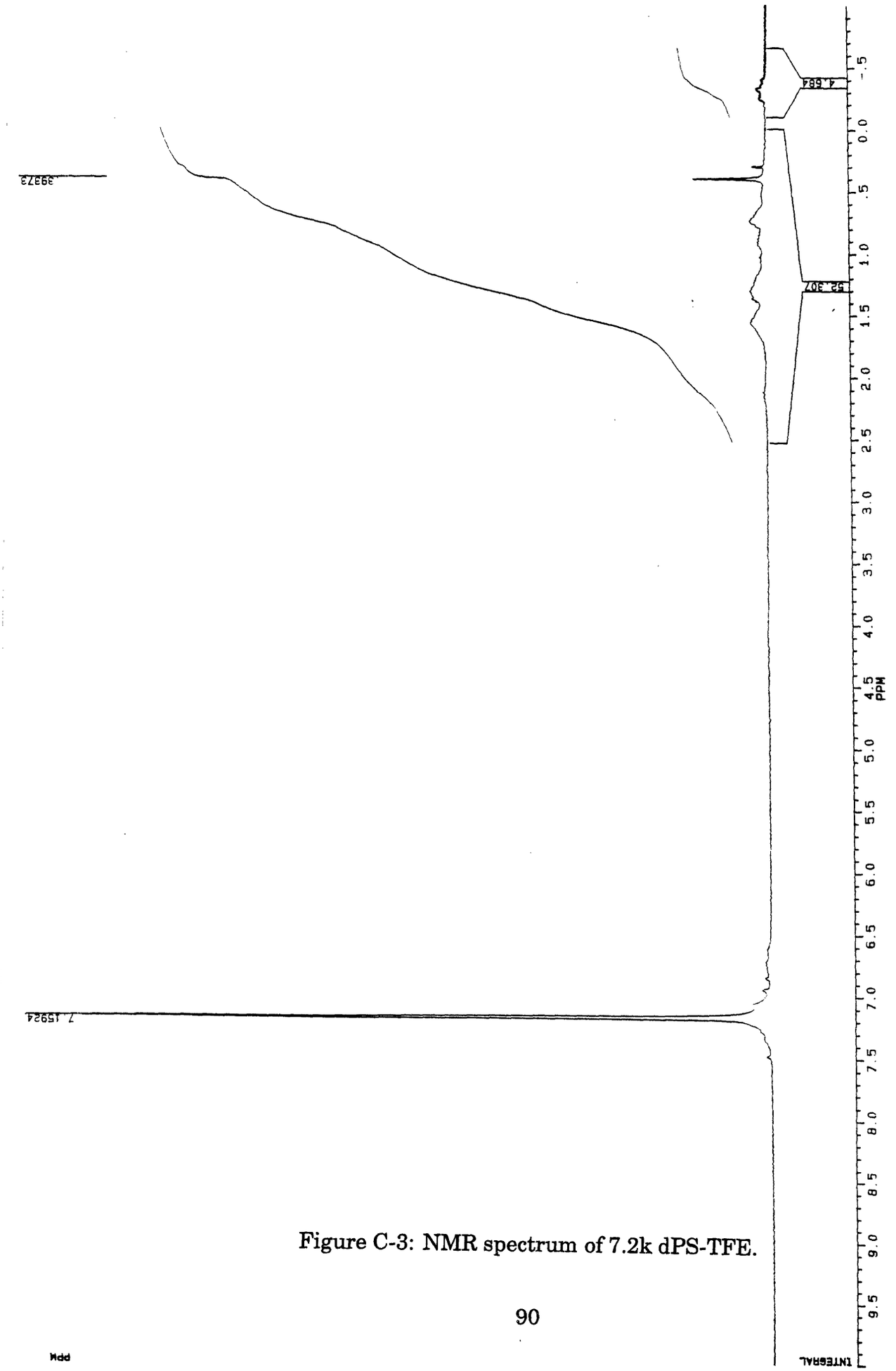

Figure C-3: NMR spectrum of 7.2k dPS-TFE.

Bibliography

[1] William J. Ward and Thomas J. McCarthy. Surface Modification. In Jacqueline I. Kroschwitz, editor, *Encyclopedia of Polymer Science and Engineering*, pages S:674–89. John Wiley and Sons, New York, second edition, 1989.

[2] Terrence G. Vargo, Patrick M. Thompson, Louis J. Gerenser, Robert F. Valentini, Patrick Aebischer, Daniel J. Hook, and Joseph A. Gardella. Monolayer Chemical Lithography and Characterization of Fluoropolymer Films. *Langmuir*, 8:130, 1992.

[3] C. Y. Kim, J. Evans, and D. A. I. Goring. Corona-Induced Autohesion of Polyethylene. *Journal of Applied Polymer Science*, 15:1365, 1971.

[4] X. D. Feng, Y. H. Sun, and K. Y. Qin. Reactive Site and Mechanism of Graph Copolymerization onto Poly(ether urethane) with Ceric Ion as Initiator. *Macromolecules*, 16:2105, 1985.

[5] Maria Liouni, Costas Touloupis, Nikos Hadjichristidis, Sotiris Karvounis, and Elizabeth Varriano-Marston. Graft Copolymerization of Methacrylates onto Wool Fibers. *Journal of Applied Polymer Science*, 45:2199, 1992.

[6] M. Tsukada, Y. Goto, G. Freddi, and H. Shiozaki. Chemical Modification of Silk with Aromatic Acid Anhydrides. *Journal of Applied Polymer Science*, 45:1189, 1992.

[7] J. F. Silvain, J. J. Ehrhardt, and P. Lutgen. Interfacial Analysis of Al and Cu Thin-Films Evaporated on Polyethylene-Terephthalate. *Thin Solid Films*, L5:195, 1991.

[8] D. Briggs, D. M. Brewis, and M. B. Konieczko. X-ray photoelectron spectroscopy studies of polymer surfaces. Part 3 Flame treatment of polyethylene. *Journal of Materials Science*, 14:1344, 1979.

[9] Souheng Wu. *Polymer interface and adhesion*, chapter 5, Surface Tension and Polarity of Solid Polymers. Marcel Dekker, Inc., 1982.

[10] J. F. Elman, B. D. Johs, T. E. Long, and J. T. Koberstein. A Neutron Reflectivity Investigation of Surface and Interface Segregation of Polymer Functional End Groups. *Macromolecules*, 27:5341–9, 1994.

[11] J. M. DeSimone, Zihibin Guan, and C. S. Elsbernd. Synthesis of Fluoropolymers in Supercritical Carbon Dioxide. *Science*, 257:945–7, August 1992.

[12] Karen Celia Fox. Cleaner Manufacturing of Plastics — With a Bit of Bubbly. *Science*, 265:321, July 1994.

[13] J. M. DeSimone, E. E. Maury, Y. Z. Menceloglu, J. B. McClain, T. J. Romack, and J. R. Combes. Dispersion Polymerizations in Supercritical Carbon Dioxide. *Science*, 265:356–9, July 1994.

[14] P.-G. de Gennes. Mechanical properties of polymer interfaces. In I. C. Sanchez, editor, *Physics of Polymer Surfaces and Interfaces*, chapter 3, pages 55–71. Butterworth–Heinemann, Boston, first edition, 1992.

[15] Xin Chen and Joseph A. Gardella. Surface Modification of Polymers by Blending Siloxane Block Copolymers. *Macromolecules*, 27:3393–9, 1994.

[16] Paul J. Flory. *Principles of Polymer Chemistry*. Cornell University Press, 1953, Fifteenth printing 1992.

[17] Pierre-Gilles de Gennes. Tension superficielle des polymeres fondus (Surface tension of a molten polymer). *Comptes Rendus de l Academie des Sciences Serie II — Mechanique Physique Chimie Sciences de L Univers Sciences de la Terra*, 307:1841–4, 1988.

[18] Doros N. Theodorou. Microscopic Structure and Thermodynamic Properties of Bulk Copolymers and Surface-Active Polymers at Interfaces. 2. Results for Some Representative Chain Architectures. *Macromolecules*, 21:1422, 1988.

[19] Jonathan G. Harris. Liquid–Vapor Interfaces of Alkane Oligomers. Structure and Thermodynamics from Molecular Dynamics Simulations of Chemically Realistic Models. *The Journal of Physical Chemistry*, 96(12):5077–86, December 1992.

[20] R. G. Winkler, T. Matsuda, and D. Y. Yoon. Stochastic dynamics simulations of polymethylene melts confined between solid surfaces. *The Journal of Chemical Physics*, 98(1):729–36, January 1993.

[21] Michele Vacatello, Do Y. Yoon, and Bernard C. Laskowski. Molecular arrangements and conformations of liquid n-tridecane chains confined between two hard walls. *Journal of Chemical Physics*, 93:779, 1990.

[22] Gregory F. Meyers, Benjamin M. DeKoven, and Jerry T. Seitz. Is the Molecular Surface of Polystyrene Really Glassy? *Langmuir*, 8:2330–2335, 1992.

[23] Anne M. Mayes. Glass transition of amorphous polymer surfaces. *Macromolecules*, 27:3114–5, 1994.

[24] W. Zhao, X. Zhao, M.H. Rafailovich, J. Sokolov, R.J. Composto, S.D. Smith, M. Satkowski, T.P. Russell, W.D. Dozier, and T. Mansfield. Segregation of Chain Ends to Polymer Melt Surfaces and Interfaces. *Macromolecules*, 26:561–2, 1993.

[25] A. M. Botelho do Rego, J. D. Lopes da Silva, M. Rei Vilar, M. Schott, S. Petitjean, and R. Jérôme. End Chain Segregation Effects in Polymer Surfaces Observed by HREELS: A Preliminary Study. *Macromolecules*, 26:4986–8, 1993.

[26] S. Affrossman, M. Hartshorne, R. Jerome, R. A. Pethrick, S. Petitjean, and M. Rei Vilar. Surface Concentration of Chain Ends in Polystyrene Determined by Static Secondary Ion Mass Spectroscopy. *Macromolecules*, 26:6251–4, 1993.

[27] Thomas G. Fox and Paul J. Flory. The Glass Temperature and Related Properties of Polystyrene. Influence of Molecular Weight. *The Journal of Polymer Science*, 14:315, 1954.

[28] T. G. Fox and S. Loshaek. Influence of Molecular Weight and Degree of Crosslinking on the Specific Volume and Glass Temperature of Polymers. *The Journal of Polymer Science*, 15:371, 1955.

[29] Cathy A. Fleisher, Jeffrey T. Koberstein, V. Krukonis, and P. A. Wetmore. The Effect of End Groups on Thermodynamics of Immiscible Polymer Blends. 1. Interfacial Tension. *Macromolecules*, 26:4172–8, 1993.

[30] D. G. Legrand and G. L. Gaines. The Molecular Weight Dependence of Polymer Surface Tension. *The Journal of Colloid and Interface Science*, 31:162, 1969.

[31] D. Legrand and G. Gaines. Surface Tension of Homologous Series of Liquids. *The Journal of Colloid and Interface Science*, 42:181, 1973.

[32] Spiros H. Anastasiadis, Irena Gancarz, and Jeffrey T. Koberstein. Interfacial Tension of Immiscible Polymer Blends: Temperature and Molecular Weight Dependence. *Macromolecules*, 21:2980, 1988.

[33] L. J. Norton, V. Smigolova, M. U. Pralle, A. Hubenko, K. H. Dai, E. J. Kramer, S. Hahn, C. Berglund, and B. DeKoven. Effect of End-Anchored

Chains on the Adhesion at a Thermoset–Thermoplastic Interface. *Macromolecules*, 28:1999–2008, 1995.

[34] Ludwik Leibler, Henri Orland, and John C. Wheeler. Theory of critical micelle concentration for solutions of block copolymers. *The Journal of Chemical Physics*, 79(7):3550, October 1983.

[35] Anne M. Mayes and Monica Olvera de la Cruz. Cylindrical versus Spherical Micelle Formation in Block Copolymer/Homopolymer Blends. *Macromolecules*, 21:2543, 1988.

[36] Harry R. Allcock and Frederick W. Lampe. *Contemporary Polymer Chemistry*, chapter 13, Kinetics of Ionic Polymerization. Prentice-Hall, Inc, 1981.

[37] George Odian. *Principles of Polymerization*, chapter 5-3, Anionic Polymerization of the Carbon-Carbon Double Bond. John Wiley & Sons, Inc., 1991.

[38] R.J. Young and P.A. Lovell. *Introduction to Polymers*, chapter 4, Structure. Chapman & Hall, 1991.

[39] Edward A. Collins, Jan Bareš, and Fred W. Billmeyer. *Experiments in Polymer Science*, chapter 7. John Wiley & Sons, 1973.

[40] J. L. McNaughton and C. T. Mortimer. Differential Scanning Calorimetry. Perkin Elmer, Norwalk, CT, 1975.

[41] Doris L. Lee. Chain End Segregation in End-Labeled Polystyrenes. Bachelor's Thesis, Massachusetts Institute of Technology, 1994.

[42] A. Lee Smith. *Applied Infrared Spectroscopy*, chapter 6, Quantitative Applications. John Wiley & Sons, Inc., 1979.

[43] F. A. Bovery and L. W. Jelinski. Nuclear Magnetic Resonance. In Jacqueline I. Kroschwitz, editor, *Encyclopedia of Polymer Science and Engineering*, pages 254–325. John Wiley and Sons, New York, second edition, 1989.

[44] D. Briggs and M. P. Seah. *Practical Surface Analysis by Auger and X-ray Photoelectron Spectroscopy*. John Wiley & Sons, 1983.

[45] Walter Klöpffer. *Introduction to Polymer Spectroscopy*. Springer-Verlag, 1984.

[46] Jeffrey T. Koberstein. Interfacial Properties. In Jacqueline I. Kroschwitz, editor, *Encyclopedia of Polymer Science and Engineering*, pages 8: 237–279. John Wiley and Sons, New York, second edition, 1987.

[47] Thomas P. Russell. X-ray and neutron reflectivity for the investigation of polymers. *Materials Science Reports*, 5:171 – 271, 1990.

[48] Richard A. L. Jones, Laura J. Norton, Kenneth R. Shull, Edward J. Kramer, Gian P. Felcher, Alamgir Karim, and Lewis J. Fetters. Interfacial Segment Density Profiles of End-Anchored Polymers in a Melt. *Macromolecules*, 25:2359–2368, 1992.

[49] Samuel A. Werner and Anthony G. Klein. Neutron Optics. In David L. Price and Kurt Sköld, editors, *Neutron Scattering*, number 23 in Methods of Experimental Physics, pages 259–337. Academic Press, New York, 1989.

[50] M. Born and E. Wolf. *Principles of Optics*. Pergamon Press: Oxford, 1975.

[51] M. O. Hunt, A. Belu, R. Linton, and J. M. DeSimone. End-Functionalized Polymers. 1. Synthesis and Characterization of Perfluoroalkyl-Terminated Polymers via Chlorosilane Derivatives. *Macromolecules*, 26:4854–9, 1993.

[52] William R. Peterson, Roy Anderson, and Gerald L. Larson. Silane Blocking Agents. In *Silicon Compounds: Register and Review*. Hüls America Inc., 1991.

[53] William A. Levinson, Anthony Arnold, and Ofelia Dehodgins. Spin Coating Behavior of Polyimide Precursor Solutions. *Polymer Engineering and Science*, 33(15):980, mid-August 1993.

[54] Claire Anne Jalbert. *Surface and Interfacial Segregation in End Functionalized Polymers (Surface Tension)*. PhD thesis, University of Connecticut, 1993.

[55] Carleton Sperati. Physical Constants of Fluoropolymers. In J. Brandrup and E. H. Immergut, editors, *Polymer Handbook*, pages V/35–44. John Wiley & Sons, New York, third edition, 1989.

[56] Richard A. L. Jones, Edward J. Kramer, Miriam H. Rafailovich, Jonathon Sokolov, and Steven A. Schwartz. Surface Enrichment in an Isotopic Polymer Blend. *Physical Review Letters*, 62:280, 1989.